DEVELPOMENT OF AN ELECTRONICALLY CONTROLLED COLD PLASMA REFORMER FOR HYDROGEN HARVEST FROM BIO-FUELS

by

JOB BRUNET

Presented to the Faculty of the Graduate School of
The University of Texas at Arlington in Partial Fulfillment
of the Requirements
for the Degree of

MASTER OF SCIENCE IN ELECTRICAL ENGINEERING

THE UNIVERSITY OF TEXAS AT ARLINGTON
August 2010

ACKNOWLEDGEMENTS

I would like to thank my graduate advisor, Dr. Babak Fahimi, for his endless patience and sound advice throughout the researching and writing of this thesis.

I would like to thank my committee members, Dr. Wei-Jen Lee and Dr. William Dillon for their valuable time and support.

I would also like to thank my family and friends for their loving support and encouragement.

July 8, 2010

ABSTRACT

DEVELPOMENT OF AN ELECTRONICALLY CONTROLED COLD

PLASMA REFORMER FOR HYDROGEN

HARVEST FROM

BIO-FUELS

Job Brunet, M.S.

The University of Texas at Arlington, 2010

Supervising Professor: Babak Fahimi

The energy demand on the world market due to the limited resources has forced governments and scientists to find an alternative source of fuel to ease the burden on its populous and environment. Moreover, the rate of global warming is increasing with the rate of carbon dioxide released from emissions from coal burning power plants and also from vehicle exhaust. This trend of burn now and fix later has to end and a new source of fuel must be developed. Wind, solar, and even nuclear are great substitutes for reducing the global pollution but a new tangible fuel is required. Hydrogen is an excellent energy carrier and offers higher energy density per mass than gasoline and yields zero emission in the combustion process and with the recent development of fuel cell technologies, hydrogen is emerging as an attractive alternative fuel for energy applications. In this thesis, several hydrogen production methods are reviewed and the importance of cold plasma hydrogen reformer is addressed. Two different converter topologies are investigated and evaluated with iterative experimental approaches.

TABLE OF CONTENTS

ACKNOWLEDGEMENTS iii

ABSTRACT iv

LIST OF ILLUSTRATIONS vii

LIST OF TABLES ix

Chapter Page

1. INTRODUCTION 1

1.1 Motivation 1

1.2 Fuel Cells Applications in Automotive and Renewable Energy Systems 4

1.2.1 On Board Vehicular Prouction of Hydrogen 5

1.2.2 On Board Enrichment of Fuel for Better Efficiency 6

1.3 Historical Background on Cold Plasma and its Applications 7

1.3.1 Characterization of Plasma 7

1.3.2 Plasma Parameters 10

1.3.3 Cold Plasma 11

1.4 Objective of this Thesis 12

2. HYDROGEN HARVESTING 13

2.1 Enthalpy 14

2.2 Steam Reforming 15

2.3 Partial Oxidation Reforming 17

2.4 Autothermal Reforming 18

2.5 Plasma Reforming 19

2.5.1 DC Discharge 21

2.5.2 AC Discharge 22

2.5.3 Pulsed Discharges 23

2.5.4 Production using Beams 23

3. DEVELOPMENT OF POWER ELECTRONIC DRIVE FOR COLD PLASMA CHAMBER 25

3.1 Buck/Full Bridge 27

3.1.1 Buck Converter 27

3.1.2 Full Bridge 30

3.1.3 Low Frequency Hardware 34

3.1.4 High Frequency Transformer 37

3.2 Flyback Converter 37

3.2.1 Flyback Hardware Setup 43

4. SUMMARY AND FUTURE WORK 45

4.1 Buck Converter and Full Bridge 46

4.2 Arc Detection 47

4.3 Low Frequency Transformer 49

4.4 High Frequency Transformer 50

4.5 Flyback Converter 51

4.6 Conclusion 54

4.7 Future Work 55

REFERENCES 57

BIOGRAPHICAL INFORMATION 59

LIST OF ILLUSTRATIONS

Figure Page

1.1 Projected energy demands (left) and carbon dioxide emissions (right) projections for 2006. Source: Energy Information Administration 1

1.2 (a) Trend of CO_2 concentrations in the atmosphere, (b) average global surface temperatures. Source Fay and Golomb (2002) 2

1.3 Carbon dioxide emission distributions from 1980 to 1999 [3] 3

1.4 Evolution of carbon emission from 1975 to 2000 [3]. 3

1.5 (a) Schematic of Onboard vehicular production of hydrogen, and (b) Onboard enrichment of fuel for better efficiency. 6

1.6 Particle paths in a neutral gas and under collective behavior in plasma: (a) Brownian motion of a neutral gas molecule; (b) motion of a charged particle in plasma 8

2.1 Schematic of idealized fuel processors, showing feeds and products from steam reforming 17

2.2 Schematic of idealized fuel processors, showing feeds and products from partial oxidation reforming 18

2.3 Schematic of idealized fuel processors, showing feeds and products from autothermal reforming. 19

2.4 The characteristic curve of a DC glow discharge. 21

3.1 Cold plasma chamber configuration. 26

3.2 (top) Buck converter and full-bridge configuration. (left) switch closed. (right) switch open. 28

3.3 Buck converter waveforms. (a) Inductor voltage. (b) Inductor current. (c) Capacitor current. 30

3.4 (a) Full bridge converter. (b) S1 and S2 closed. (c) S3 S4 closed. (d) S1 and S3 closed. (e) S2 and S4 closed 31

3.5 Buck convert and full bridge experiment hardware 35

3.6 Buck converter and full bridge with the low frequency transformer 35

3.7 (a) Dial in frequency and duty cycle on bread board. (b) on proto board. (c) Implemented with the complete system36

3.8 (left) Buck converter and full bridge connected to the high frequency transformers. (right) high frequency transformer.....37

3.9 Flyback converter circuit. 38

3.10 Flyback with arc showing rise time and fall time of the secondary voltage.....44

3.11 Flyback and transformer hardware. 44

4.1 Buck converter plus inverter with a low frequency transformer schematic. 46

4.2 Ideal equivalent circuit of the high voltage/high frequency 47

4.3 (left) Current signature in the absence of an arc, (right) Current signature in the presence of an arc.....49

4.4 Low frequency full bridge converter primary voltage and current 50

4.5 High frequency transformer results: 75% duty cycle with 12.5kHz switching frequency.....51

4.6 Flyback converter with no arc. 53

4.7 Flyback converter with arc. 54

4.8 Schematic of magnetically enhanced plasma chamber.....56

LIST OF TABLES

Table Page

2.1 Thermodynamic Quantities for selected substances at 298.15 K (25 ℃).....15

CHAPTER 1

INTRODUCTION

1.1 Motivation

The energy demand on the world market due to the limited resources has forced governments and scientists to find an alternative source of fuel to ease the burden on its populous and environment. A study done by the Energy Information Administration (EIA), figure 1.1, shows the projection of energy demands and the production of carbon dioxide for the next 20 years [1].

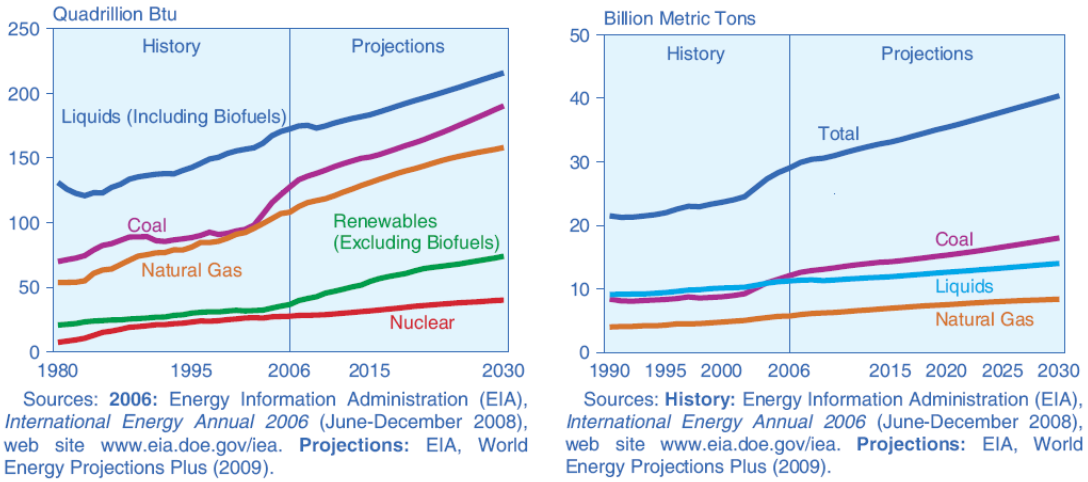

Figure 1.1 Projected energy demands (left) and carbon dioxide emissions (right) projections for 2006. Source: Energy Information Administration

The rate of global warming is increasing with the rate of carbon dioxide released from emissions from coal burning power plants and also from vehicle exhaust. As shown in figure 1.2(a), the amount of CO_2 released after the 1800's shows an exponential increase and comparing figure 1.2(b) with 1.2(a) the average global surface temperature follows the increasing CO_2 concentration. The increase injection of carbon dioxide into the atmosphere has a direct link to global warming [2].

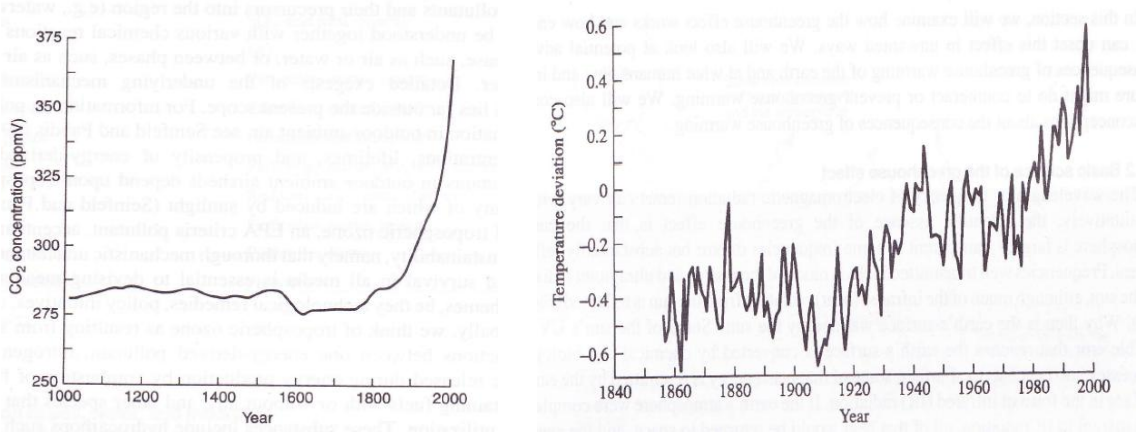

(a) (b)

Figure 1.2 (a) Trend of $\boldsymbol{CO_2}$concentrations in the atmosphere, (b) average global surface temperatures. Source Fay and Golomb (2002)

The two main causes for the increase in carbon dioxide are industries and the transportation sector. Industries are responsible for 34% of the CO_2 while the transportation sector is at 32% as illustrated in figure 1.3. In figure 1.4 shows the trend of carbon dioxide emissions and the transportation sector is a major contributor of the CO_2emissions [3].

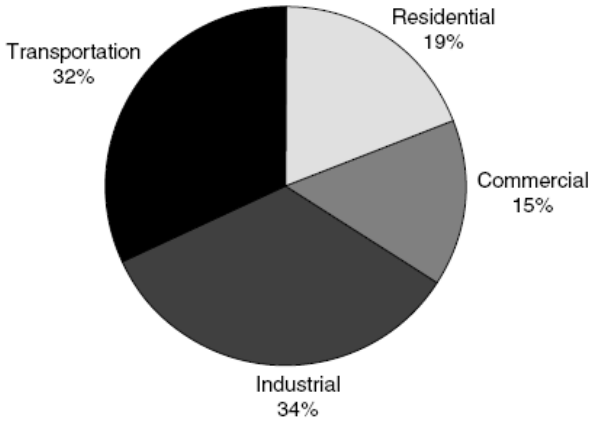

Figure 1.3 Carbon dioxide emission distributions from 1980 to 1999. [3]

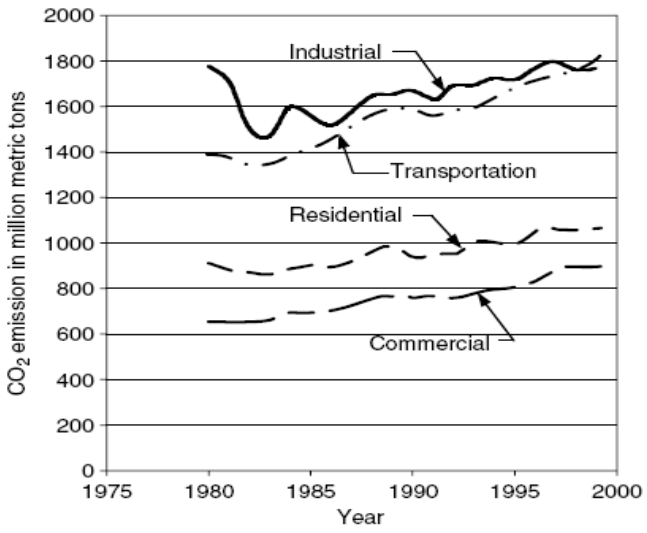

Figure 1.4, Evolution of carbon emission from 1975 to 2000. [3]

This trend of burn now and fix later has to end and a new source of fuel must be developed. Some alternatives to the increasing threat are alternative energy or sustainable

energy. Wind, solar, and even nuclear are great substitutes for reducing the global pollution but a new tangible fuel is required, one that can used on demand and supplied as needed.

Hydrogen is an energy carrier and offers higher energy density per mass than gasoline and yields zero emission in the combustion process and with the recent development of fuel cell technologies, hydrogen is emerging as an attractive alternative fuel for energy applications. There are many techniques for harvesting hydrogen, electrolysis, steam reforming (SR), partial oxidation (PO), and autothermal reforming (ATR). These techniques are inefficient and use large scale chemical plants to produce hydrogen, which makes them unsuitable for vehicle applications. A new technology must be developed to harvest hydrogen quickly, more efficiently and most of all economically.

The current technology of cold plasma reforming is smaller and compact making it ideal for automotive applications. Cold plasma can be used to reform bio-fuels such as ethanol to harvest hydrogen. The principle behind using cold plasma is to inject a hydrocarbon rich fuel into a reformer. The plasma discharge inside the reformer then releases a high amount of electrons and ions that collide with the large molecules of ethanol.

In order to develop cold plasma technology, two different types of power electronics circuits were tested with the hydrogen reformer chamber. First circuit used was a buck converter and full bridge. The second was the fly back converter.

In this thesis, the two topologies will be disguised and results for each are given. Also a discussion on what research should be done to continue the search for an alternative fuel.

1.2 Fuel Cells Applications in Automotive and Renewable Energy Systems

Hydrogen fuel cells theoretically have higher energy efficiency than internal combustion engines and they produce no direct greenhouse gas emissions. This makes them more

applicable for small scale power generation, for example, automotive and mobile power stations. Hydrogen harvesting is a key factor in successful commercial development of fuel cell technology. The lack of transportation infrastructure (refueling stations) and effective storage for hydrogen makes large scale hydrogen production plants unattractive for fuel cell application. A small scale, onboard hydrogen reformer has been recognized as an attractive alternative. Bio-ethanol is a good clean, renewable candidate for hydrogen production because it is non-toxic and easy for transportation and storage [4].

1.2.1 On Board Vehicular Production of Hydrogen

Using cold plasma reforming for onboard vehicular production of hydrogen is one method of resolving the issues of storage and transporting hydrogen. Figure 1.5(a) shows the setup of how a cold plasma reformer would be used for onboard vehicular application. First the ethanol in the fuel tank would enter the fuel reformer, hydrogen and carbon dioxide would be produced. The carbon dioxide from the reformer would be filtered leaving only the hydrogen to be used in the fuel cell. Power generated by the PEM fuel cell would be used to run a motor. Also part of that power would condition through a power supply to run the fuel reformer [5].

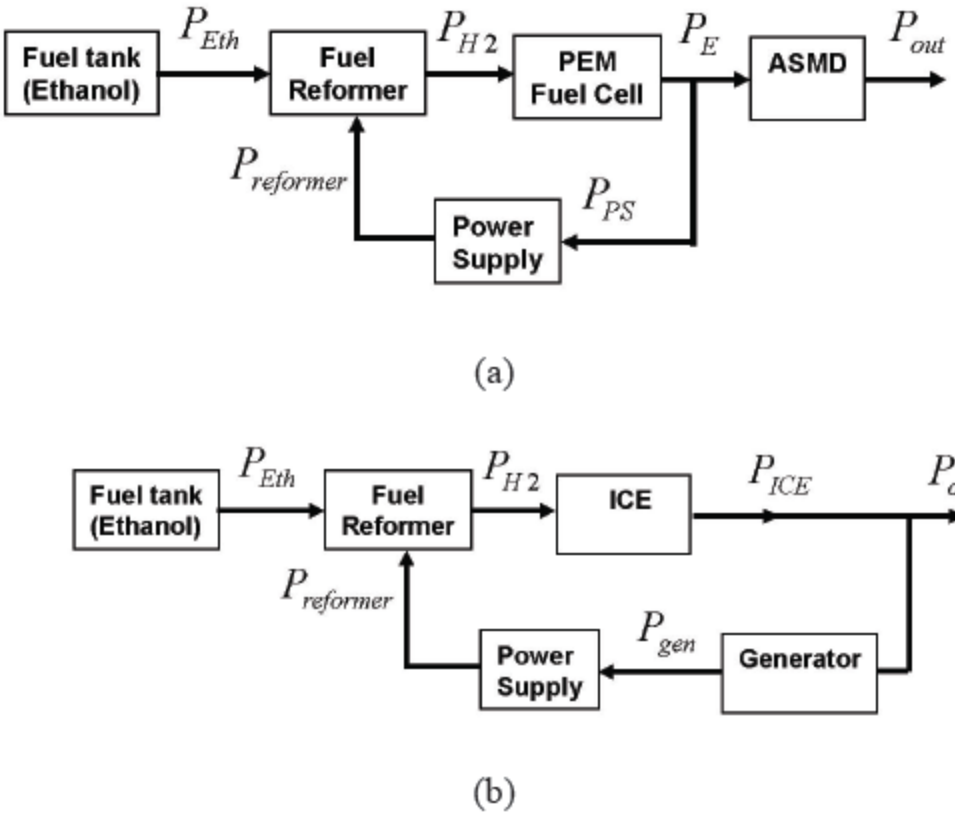

Figure 1.5 (a) Schematic of onboard vehicular production of hydrogen, and (b) onboard enrichment of fuel for better efficiency.

1.2.2 On Board Enrichment of Fuel for Better Efficiency

In figure 1.5(b) illustrates the arrangement of an onboard enrichment of fuel for better efficiency for vehicular applications. Ethanol from the fuel tank would enter the cold plasma reforming and be converted to hydrogen and carbon dioxide. From the fuel reforming it would go directly into the internal combustion engine to be used to enrich the fuel of the vehicle. Also part of the power generated from the ICE would back to supply power to the reformer [5].

1.3 Historical Background on Cold Plasma and its Applications

1.3.1 Characterization of Plasma

Low-pressure plasma, cold plasma, non-equilibrium plasma, and glow discharge are some of the terms that used to describe the same type of plasma process. The technologies that are using plasma processes are plasma assisted chemical vapor deposition (PACVD), plasma enhanced chemical vapor deposition (PECVD, ionitriding, and plasma etching [6].

Plasma chemistry takes place under non-equilibrium conditions, and the reaction occur while the gases are exposed to cold plasma and remain at relatively low temperatures. Cold plasma is similar to that occurring in fluorescent bulbs or neon lights which are an electrical discharge in a gas at low temperature. The phenomenon occurring in cold plasmas are complex and are not fully understood but it is possible with the current knowledge of plasma physics and chemistry to adjust and control the composition of the gas mixtures and the parameters of the discharge to achieve the desired results for hydrogen reforming [6].

Plasma is the fourth state of matter, apart from solid, liquid or gas but in a rigorous way, plasma can be defined as a quasi-neutral gas of charged and neutral particles characterized by a collective behavior. The collective behavior of a neutral gas is described by the kinetic theory of gases. While in an ordinary neutral gas no forces act between the molecules of the gas and the particles travel in straight lines, with a distribution of velocities. The motion of the molecules is controlled by the collision among themselves and with the walls of the container. As a result of these collisions, the molecules of a neutral gas follow a random Brownian motion, as illustrated in figure 1.6 [6].

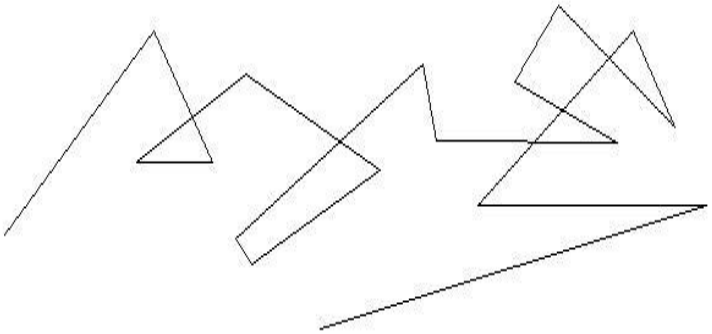

(a)

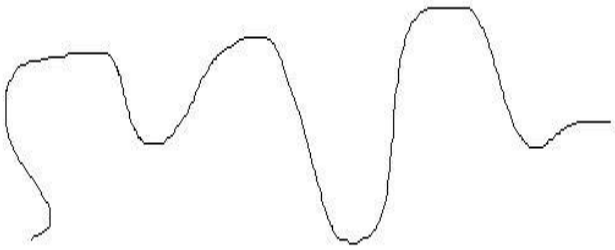

(b)

Figure 1.6 Particle paths in a neutral gas and under collective behavior in plasma: (a) Brownian motion of a neutral gas molecule; (b) motion of a charged particle in plasma.

If the particles of the neutral gas are considered to be a rigid sphere of radius r and their density n, the kinetic theory of the gases defines the cross section for collision, σ and mean free path, λ, as

$$\sigma = \pi r^2 \tag{1.1}$$

$$\lambda = \frac{1}{\sigma n} \tag{1.2}$$

The average number of collisions per second, called the collision frequency, v, and the mean time between collisions, τ, are given by

$$v = \frac{\bar{v}}{\lambda} \tag{1.3}$$

$$\tau = \frac{1}{v} = \frac{\lambda}{\bar{v}} \tag{1.4}$$

Where $\bar{v}$ the average velocity of the molecules in the gas which is determined by the temperature, T:

$$\bar{v} = \left(\frac{kT}{M}\right)^{1/2} \tag{1.5}$$

M is the mass of the molecule, and k is the Boltzmann constant. If the temperature of the gas is constant, then the coalitional mean free path is inversely proportional to the pressure in the system:

$$\lambda = \frac{ct}{p} \tag{1.6}$$

Where ct = a constant depending of the gas and p = pressure in the gas [6].

In plasma, the motion of the particles can cause local concentrations of positive and negative electric charges. The concentrations of charges create long-ranged Coulombic fields that affect the motion of charged particles far away from the charge concentrations. The elements of the plasma affect each other, even at large separations, giving the plasma its

characteristic collective behavior. A charged particle in plasma moves along a path which on average follows the electric field. This path is illustrated in figure 1.6(b) [6].

1.3.2 Plasma Parameters

Plasma that is sustained in a mixture of molecular gases, contain a variety of different neutral and charged particles. The plasma can be characterized by the some basic parameters [6]:

- The density of the neutral particles.
- The densities of the electrons and ions.
- The energy distributions of the neutral particles, ions, and electrons.

The plasma density is an important parameter in the plasma process because the efficiency of the processes occurring in the plasma and their reaction rates are generally dependent directly on the density of the charged particles [6]. Electrons are the main particles that transfer energy from the external electric field to the discharge gas. Both electrons and ions are electrically charged and accelerated by absorbing energy from the applied external field. Because of the light weight of the electron compared to the ions, the electron absorbs the majority of the energy and accelerates much more than the ions. The collision of accelerated electrons and large gas molecules make them ionized, so the more accelerated and energized electrons in the gas the higher the efficiency. There are a number of methods to produce plasmas mechanically, applied pressure and electrode geometry can be classified as follows [5,6]:

- Combustion
- Flames
- Electrically heated furnaces

- Electric discharges (corona, spark, glow, arc, microwave discharges, plasma jets and radio frequency)
- Shocks (electrically, magnetically and chemically driven)

Because of the different plasma parameters, plasma can be classified into three groups.

- Complete thermodynamic equilibrium (CTE) – exists in stars and short intervals of a strong explosions.
- Local thermodynamic equilibrium (LTE) – exist under two circumstances: very high energetic heavy particles at temperatures of $10^6 - 10^8\ °K$ and atmospheric pressure even at temperatures of $6000\ °K$.
- Non LTE plasma, also called cold plasma which the electrons can reach a temperature range of $10^4 - 10^5\ °K$ while the gas around the plasma can be as low as room temperature.

All three plasmas described above are comparable at producing the same amount of hydrogen but the energy demand for cold plasma is significantly less. Plasma can replace catalysis and accelerates chemical reactions because of the high temperature effect. The advantages of using plasma are extremely high productivity of apparatus, low investment and operation cost [5, 6].

1.3.3 Cold Plasma

Certain restriction for high energy consumptions applies to some applications of thermal plasma approach. Also the use of high current operation results in high electrode wear. Cold plasmas have been used for fuel gas treatment and shows potential for organic synthesis because of non-equilibrium properties, low power requirements and its capacity to induce physical and chemical reactions within gases at relatively low temperatures [5, 8]. The electrons

in cold plasma can reach temperatures in the range of $10^4 - 10^5\ °K$ so they are very energetic while the gas temperature remains at room temperature. High electron temperature and high energy, determines the unusual chemistry of cold plasmas [5, 8]. This removes the necessity to preheat feed streams. As mentioned before different types of cold plasma arise from the generation mechanism, applied pressure and the electrode geometry.

The most common method for plasma generation is electrical breakdown of natural gas in an external electric field. The electric discharges are classified as dc, ac and pulse discharges on the basis of electric field behavior [5, 10].

1.4 Objective of this Thesis

The objective of this thesis is to review the current techniques of large scale hydrogen reforming like steam reforming, partial oxidation, and autothermal reforming. Also this thesis will discuss the use of cold plasma for fuel reforming of ethanol and last this thesis will discuss the different power electronic converters developed to achieve the desired power to achieve the maximum hydrogen yield from the cold plasma reformer.

CHAPTER 2

HYDROGEN HARVESTING

The petrochemical industries have been producing hydrogen for decades but these methods are not compatible with the automotive industries for example [5, 12]:

- Level of production is lower by several orders of magnitude.
- Size and weight of the reformer due to automotive constraints.
- Ability to handle multiple start up and shut downs.
- Response to the change in demand which can vary from 5 to 100% of the rated processing rate.
- Strict cost factor (economical).
- Reliability in performance throughout the life cycle.

Depending on the application, Different fuels can be used to harvest hydrogen for transportation such as, ethanol, methanol, gasoline and diesel. The large scale hydrogen production plants tend to use natural gas or propane but ethanol, butane and biomass materials are also used. Some of these methods the stationary plants uses are steam reforming (SR), partial oxidation reforming (PO), and autothermal reforming (ART) [5, 12].

To better understand the physical and chemical breakdown of hydrocarbons a basic understanding of the first Law of Thermodynamic and enthalpy, which state that energy is conserved.

2.1 Enthalpy

Enthalpy is the energy that is absorbed (Endothermic) or released (exothermic) when a physical or chemical reaction takes place within a system. The majority of physical and chemical changes take place under constant pressure of Earth's atmosphere. The high energy chemical reactions will focus on is the heat transferred under the constant-pressure conditions. Enthalpy, denoted as ΔH, is the quantity that deals with the heat absorbed or released at constant pressure. Equation (2.1), describes the change in enthalpy is equaled to the enthalpy of the products minus the reactants.

$$\Delta H = \Delta H_{products} - \Delta H_{reactants} \tag{2.1}$$

An example can be give by burning hydrogen in equation (2.2). Equation (2.3) shows the enthalpy of the reactants and products which are $\Delta H_{H_2} = 0$, $\Delta H_O = 247.5\ kJ/mol$, and $\Delta H_{H_2O} = -241.82\ kJ/mol$ from table (2.1). Notice that the enthalpy of $\Delta H_{H_2} = 0$, this is due to the fact that hydrogen occurs naturally as H_2 in nature. Substituting equation (2.3) into (2.1), we get equation (2.4).

$$2H_2(g) + O_2(g) \xrightarrow{yields} 2H_2O(g), \qquad \Delta H = -483.64\ kJ/mol \tag{2.2}$$

$$2\left[\Delta H_{H_2}\right] + \left[\Delta H_{O_2}\right] \xrightarrow{yields} 2\left[\Delta H_{H_2O}\right] \tag{2.3}$$

$$\Delta H = 2\left[\Delta H_{H_2O}\right] - \left\{2\left[\Delta H_{H_2}\right] + \left[\Delta H_{O_2}\right]\right\} \tag{2.4}$$

This process is extremely exothermic by releasing -483.64 kJ of heat. Also this process is reversible due to the first law of thermodynamics, so using water to produce hydrogen would

be $\Delta H = 483.64\ kJ/mol$. This process can be used to calculate the amount of energy needed to produce hydrogen from different methods of reforming.

Table 2.1 Thermodynamic Quantities for selected substances at 298.15 K (25℃).

Carbon	∆H (kJ/mol)
C(g)	718.4
CO(g)	-110.5
CO2(g)	-393.5
Hydrocarbons	
Methanol, CH3OH(l)	-238.6
Methane, CH4(g)	-74.8
Ethanol, C2H6O(g)	-235.1
Hydrogen	
H(g)	217.94
H2(g)	0
Oxygen	
O(g)	247.5
O2(g)	0
H2O(g)	-241.82
H2O(l)	-136.1

2.2 Steam Reforming

Hydrogen is produced, when steam reacts with the fuel, such as natural gas or methane, in the presence of a catalyst. This method of reforming also produces some unwanted byproducts like carbon dioxide and carbon monoxide as shown in equation 2.5.

$$C_nH_mO_p + steam \xrightarrow{yields} CO_x + Hydrogen, \Delta H > 0 \quad (2.5)$$

The steam reformers are built for long steady-state operation and can produce high concentrations of hydrogen. Also the byproducts, carbon monoxide and carbon dioxide are removed from the reformate gas stream by variety of reactions and scrubber techniques, such as the water gas shift reaction, methanation, CO_2 absorption, and pressure swing adsorption. Steam reforming is extremely endothermic (absorbs heat), and reactor designs are limited by heat transfer. So the reactors are designed to support heat exchange and tend to be large and heavy. The indirect heat transfer makes typical steam reformers less attractive for fast startup and dynamic response needed for automotive applications [5, 12].

Equation (2.6) can be calculated by using the process as equations (2.2)-(2.4). Steam reforming of ethanol is endothermic with an enthalpy of 256 kJ/mol. Equation (2.7) shows the water gas shift which help reduce carbon monoxide by adding water and produces carbon dioxide and hydrogen. This method is commonly used in all four reforming techniques in this thesis.

$$C_2H_6O + H_2O \xrightarrow{yields} 2CO + 4H_2; \quad \Delta H = 256\ kJ/mol \tag{2.6}$$

$$CO + H_2O \xrightarrow{yields} CO_2 + H_2; \ \Delta H = -41\ kJ/mol \tag{2.7}$$

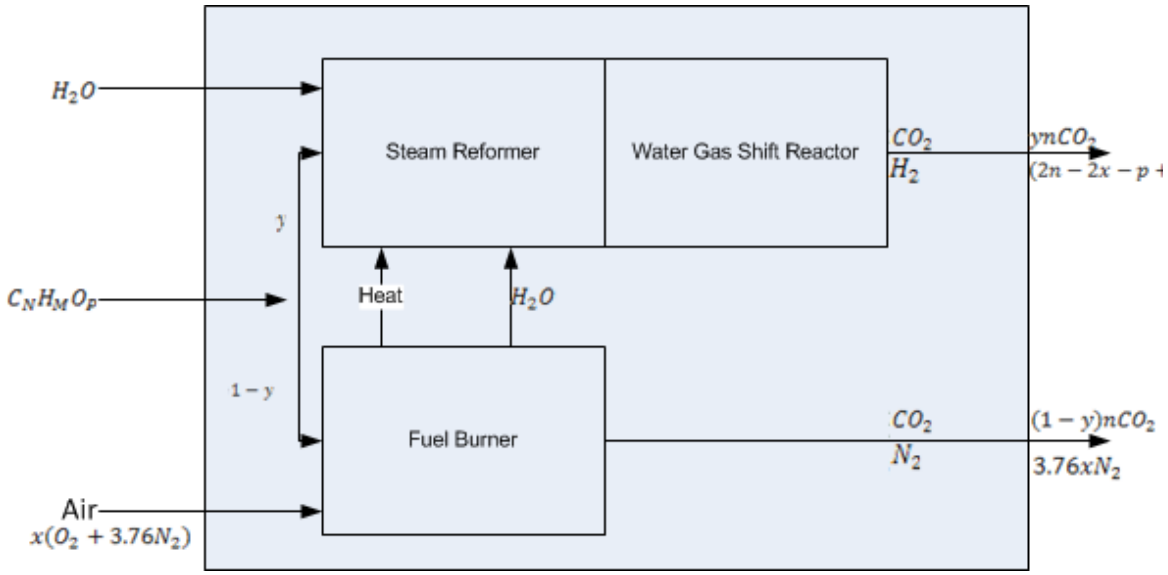

Figure 2.1 Schematic of idealized fuel processors, showing feeds and products from steam reforming.

2.3 Partial Oxidation Reforming

Partial oxidation reformers reacts the fuel with the exact proportions of oxygen. This initial oxidation results in heat generation at high temperatures.

$$C_2H_6O + \frac{1}{2}O_2 \xrightarrow{yields} 2CO + 3H_2; \quad \Delta H = 14.1\ kJ/mol \tag{2.8}$$

The heat generated from the initial oxidation reaction raises the gas temperature over 1000 degree Celsius, which helps to steam reform the remaining fuel or byproducts by adding the appropriate amount of steam into the gas mixture. With the correct amount of steam added , this procedure can be done with or without the present of a catalyst [5, 12].

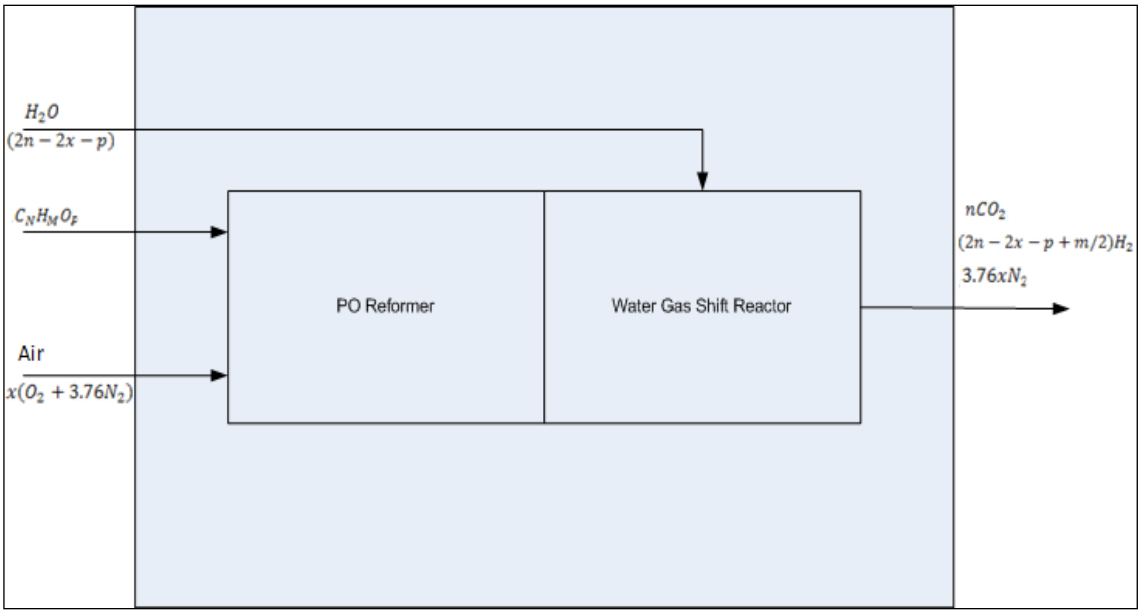

Figure 2.2 Schematic of idealized fuel processors, showing feeds and products from partial oxidation reforming.

2.4 Autothermal Reforming

Autothermal reformers combine the heat generated by Steam reforming and partial oxidation reforming by feeding the fuel, water and air together into the reactor.

$$C_nH_mO_p + air + steam \xrightarrow{yields} CO_x + hydrogen + nitrogen, \Delta H_r < 0 \qquad (2.5)$$

A catalyst is used to control the reaction pathways and thereby determine the relative extents of oxidation and steam reforming. The steam reforming reaction absorbs part of the heat generated by the oxidation reaction, limiting the maximum temperature in the reactor. This reaction results in a slight exothermic (radiates heat) process and to obtain the desired conversion and product selectivity, using the precise catalyst is essential [5, 12].

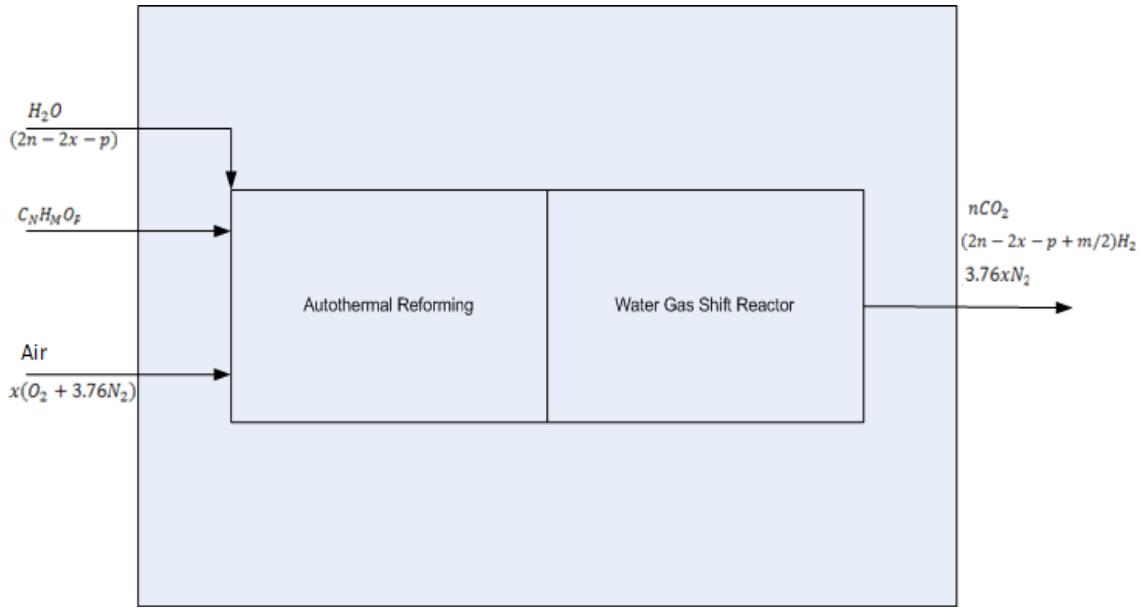

Figure 2.3 Schematic of idealized fuel processors, showing feeds and products from autothermal reforming.

2.5 Plasma Reforming

Plasma technology has advantages over conventional large scale hydrogen harvesting. Plasma assisted techniques are widely used in various industrial applications like automotive, aerospace, biomedical industries and fabrication of microelectronics components.

The downside of conventional large scale reformers are its cost, deterioration of catalysts, size, limitations on rapid response and restraints on hydrogen production from heavy hydrocarbon. Also some disadvantages are the dependence on electrical power (MW range) and difficulty of high pressure operation that increases electrode erosion due to decreased arc mobility and thus decreased electrode life time [5, 13].

Plasma devices referred to as Plasmatrons can generate very high temperatures with a high degree of control using electricity. The heat generation is independent of reaction chemistry and optimal operating conditions. Furthermore, heat generation can be maintained

over a wide range of feed rates and gas composition. Compactness is guaranteed by high energy density associated with the plasma and by reduced reaction times resulting in short residence time. The plasma conditions of high temperature and high degree of dissociation and substantial degree of ionization can be used to accelerate thermodynamically favorable chemical reactions without a catalyst or provide the energy required for endothermic reforming processes. Plasma reformers can provide number of advantages as follows:

• Compactness and lightness due to high power density

• High conversion efficiencies

• Minimal cost (simple metallic or carbon electrodes and simple power supplies)

• Fast response time (fraction of a second)

• Operation with a broad range of fuels including heavy hydrocarbons like crude oil and with dirty hydrocarbons like high sulfur diesel.

As an example one can consider methane reforming, (2.6) and (2.7) which has two stages. During the first stage complete combustion of part of methane occur producing carbon monoxide and hydrogen, substantially increasing the temperature of the system. During the second stage (water gas shift), reactions of the remaining methane with carbon monoxide and water producing carbon dioxide and hydrogen, while decreasing the temperature of the system.

The benefit of using plasma for reformation is that the reaction and water gas shift occurs in a single process. This plasma process accelerates the reactions (both by the increase in temperature to vaporize the fuel as well as by the presence of highly reactive radicals/ions preparing the hydrocarbon air mixture for the catalytic phase [5, 13]. So the plasma acts as the catalyst and the source of heat required for the reforming.

2.5.1 DC Discharges

In this method plasma is created in closed discharge vessels using internal electrodes. According to Fig. 2.4 [5, 6] based on the applied voltage and the discharge current, different discharges could be created [5, 10].

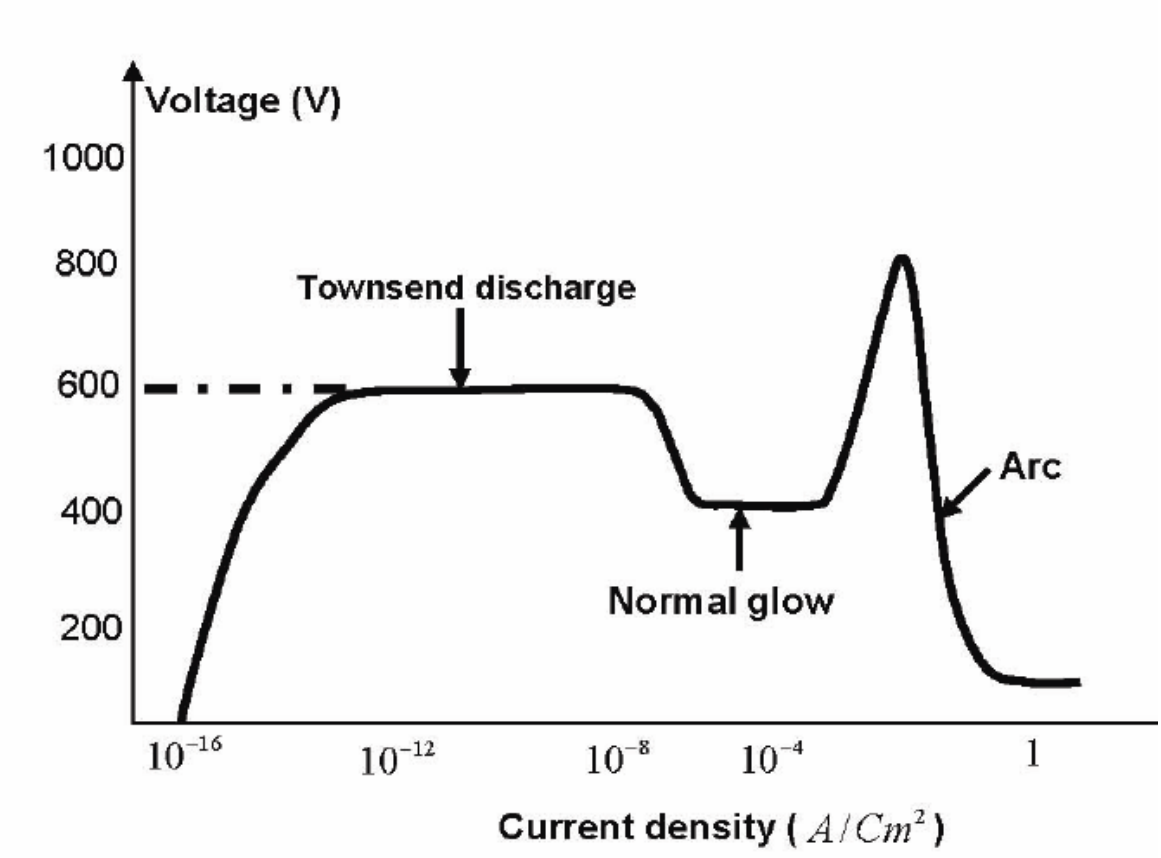

Figure 2.4 The characteristic curve of a dc glow discharge.

Based on this figure following discharges can be considered [5, 8]:

- Glow Discharge: Is a low pressure discharge (10 mbar) usually operating between flat electrodes. In this plasma the electrons are highly energetic. The excited neutral atoms

and molecules generate a typical glow like in fluorescent tubes. Because of the low pressure characteristics it is not suitable for chemical synthesis.

- Corona discharge: It is an inhomogeneous discharge and can be initiated at atmospheric pressures using inhomogeneous electrode geometries like a pointed wire electrode as anode and a plate for cathode. The small radius of curvature at the top of the electrode results in high electric field required for ionizing the neutral molecules.
- Silent or Dielectric barrier discharge (DBD): In this type a dielectric layer covers at least one electrode. The entire electrode area will be effective for discharge reaction. The discharge is initiated at any location within the gap between electrodes and the charge accumulates on the dielectric to form an opposite electric filed and interrupts the current flow in a few nanoseconds to generate micro discharges. The duration of the current pulse relates to the pressure, properties of the gases and the dielectric material applied.

2.5.2 AC Discharges

The following methods microwave discharge; radio frequency discharge and gliding arc discharge are classified as AC discharges:

- Microwave discharge: It operates at very high frequencies such as 2.45 GHz in the range of microwaves in which only light electrons can follow the oscillations of the electric field. It can be implemented over a wide range of pressure. Various types of microwave reactors are: discharges produced in closed structure, in open structure and in resonance structure with a magnetic field [5, 10].
- Radio frequency discharge: It operates at high frequencies of several MHz (1-100MHz) and very low pressures to achieve the non equilibrium condition. This type of plasma is not suitable for chemical synthesis [5, 8].

- Gliding arc discharge: It is a transitional type of atmospheric pressure arc discharges, which can provide relatively high levels of electron density, current and power-typical for thermal plasmas, together with relatively low temperature and elevated electric field typical for cold non-equilibrium plasmas. This phenomenon consists of periodic self-triggered transitions of atmospheric pressure thermal arc $(3000 - 5000\ ^\circ K)$, moving in a gas flow between divergent electrodes, into, non-thermal non-equilibrium discharge [5, 11] .

2.5.3 Pulsed Discharges

In this method, the dc pulsed discharges are used instead of continuous dc discharge. This method has advantages like higher operating power, and additional performance control by a variable duty cycle of active plasma regime and overflow and minimization of the effect like inhomogeneous thin film decomposition compared to the DC discharge [5, 10]. It must be noted that the main reaction occurs when high energy electrons are collided upon heavy molecules of hydrocarbons in the first portion of the breakdown (few tens to hundreds of nanosecond in length) [5, 10].

2.5.4 Production using Beams

This method is mainly used in material fabrication. It is frequently accomplished by the use of electron beams and laser beams. The plasma discharges generated using this method is sustainable by interaction of an electron beam with a gaseous medium. This interaction produces turbulent plasma oscillations with high amplitude. The heating of the electrons in this turbulent field is sufficient to sustain the beam produced discharged plasma. Up to 70% of the

beam energy can be transferred to the plasma. In this method it is possible to generate plasmas with high degrees of ionization in low pressure environment [5, 10].

CHAPTER 3

DEVELOPMENT OF POWER ELECTRONIC DRIVE FOR COLD PLASMA CHAMBER

The most common ways of reforming as mentioned in chapter 2 are steam reforming, partial oxidation and autothermal reforming which are all large scale industrial processes that need high amounts of power to harvests hydrogen. Cold plasma has the benefit of being smaller and light weight and coupled with power electronic has an advantage for automotive applications.

In order to make onboard cold plasma reforming possible the size and weight of the reforming must fit automotive constraints, the ability to handle multiple start up and shut down cycles, and a strict cost factor are some of the issues to make cold plasma reforming work for automotive application.

Using power electronics to create plasma is a challenge due to the high voltage needed to create an arc. The cold plasma chamber, in figure 3.1, is the setup used for this experiment.

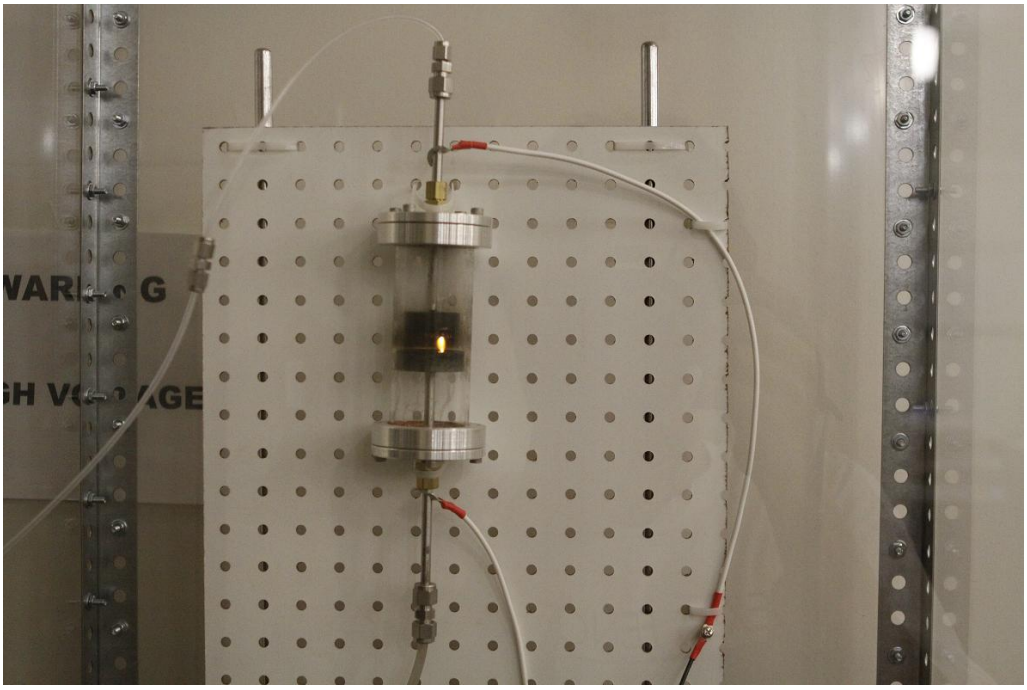

Figure 3.1 Cold plasma chamber configuration.

The electrodes are a plate to plate configuration, with a discharge gap of 10-15mm. The anode is made of stainless steel tubes, with a 1/16 inch tube inside of a 1/8 OD tube. A hollow needle with an inner diameter of 0.26 mm is put inside the 1/16 inch tube close to the tip of the tube electrode. The cathode is made of 3/8 inch OD stainless steel tube with a ½ inch OD stainless steel sintered filter cap (~90um) on the top. The porous structure of the filter cap distributes the plasma homogeneously on the cathode and allows the vapor to pass through the filter which also ensures that the entire vapor passes through the plasma zone. The reactor vessel is a 1 inch OD quartz tube. The mixture of ethanol to water is fed through the anode, and is vaporized inside of the tip of the anode before entering the plasma reaction zone for reaction. The product and unused reactants pass through the filter cap, exiting the reactor through the cathode.

3.1 Buck/Full Bridge

The first criterion in creating cold plasma is to choose a converter topology that can handle high voltage output. The target voltage output was 20kV to breakdown the discharge gap of 10-15mm. so the first prototype was a buck converter and a full bridge.

3.1.1 Buck Converter

A buck converter is a step down dc/dc converter used for stabilizing or controlling the output dc voltage. Figure 3.1(top) shows a basic dc/dc converter, in figure 3.1(left) illustrates when the switch is closed and the diode goes into reverse bias. Figure 3.1(right) shows the dc/dc converter switch open and the diode provide a path for the inductor current to flow [14].

Analyzing the buck converter when the switch is closed, figure 3.2(left) the diode is reverse biased and the voltage across the inductor is

$$v_L = V_S - V_O = L\frac{di_L}{dt} \tag{3.1}$$

$$\frac{di_L}{dt} = \frac{V_S - V_O}{L} \tag{3.2}$$

The change in inductor current is a positive constant, so the current rises linearly, as shown in figure 3.3(b). The current changes while the switch is closed are (3.4).

$$\frac{di_L}{dt} = \frac{\Delta i_L}{\Delta t} = \frac{\Delta i_L}{DT} = \frac{V_S - V_O}{L} \tag{3.3}$$

$$(\Delta i_L)_{close} = \left(\frac{V_S - V_O}{L}\right) DT \tag{3.4}$$

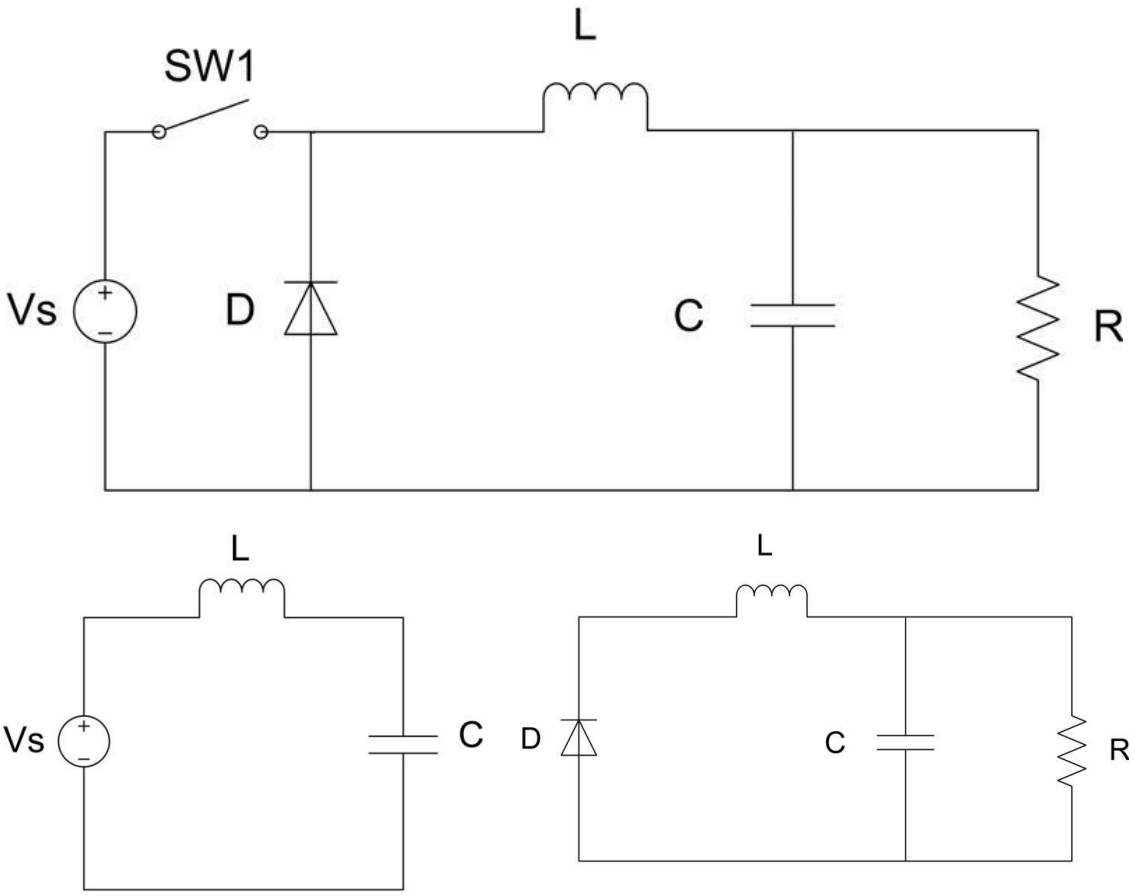

Figure 3.2 (top) Buck converter and full-bridge configuration, (left) switch closed, (right) switch open.

When the buck converter switch is open, the diode becomes forward biased to carry the inductor current, and the equivalent circuit figure 3.1(c). The voltage across the inductor is:

$$v_L = -V_O = L\frac{di_L}{dt} \tag{3.5}$$

$$\frac{di_L}{dt} = \frac{-V_O}{L} \tag{3.6}$$

The derivative of the current, equation (3.6) is a negative so the current decreases linearly, as illustrated in figure 3.3(b). When the switch is open the inductor current is equation (3.7).

$$\frac{\Delta i_L}{\Delta t} = \frac{\Delta i_L}{(1-D)T} = \frac{-V_O}{L} \tag{3.7}$$

$$(\Delta i_L)_{open} = \left(\frac{-V_O}{L}\right)(1-D)T \tag{3.8}$$

At steady state operation the inductor current at the end of the switching period must be the same as the beginning, that is the net change in inductor current over one period is zero as in equation (3.9) [14].

$$(\Delta i_L)_{closed} + (\Delta i_L)_{open} = 0 \tag{3.9}$$

$$\left(\frac{V_S - V_O}{L}\right)DT - \left(\frac{V_O}{L}\right)(1-D)T = 0 \tag{3.10}$$

Solving for $V_O$in equation (3.10), we get:

$$V_O = V_S D \tag{3.11}$$

Equation (3.11) describes the relation between the input voltage and the output voltage with a ratio D called the duty cycle. A buck converter is a dc/dc converter that steps the input voltage down controlling the energy stored in the inductor by turning on and off the switch. The duty cycle has a direct relation between the output voltage and input voltage.

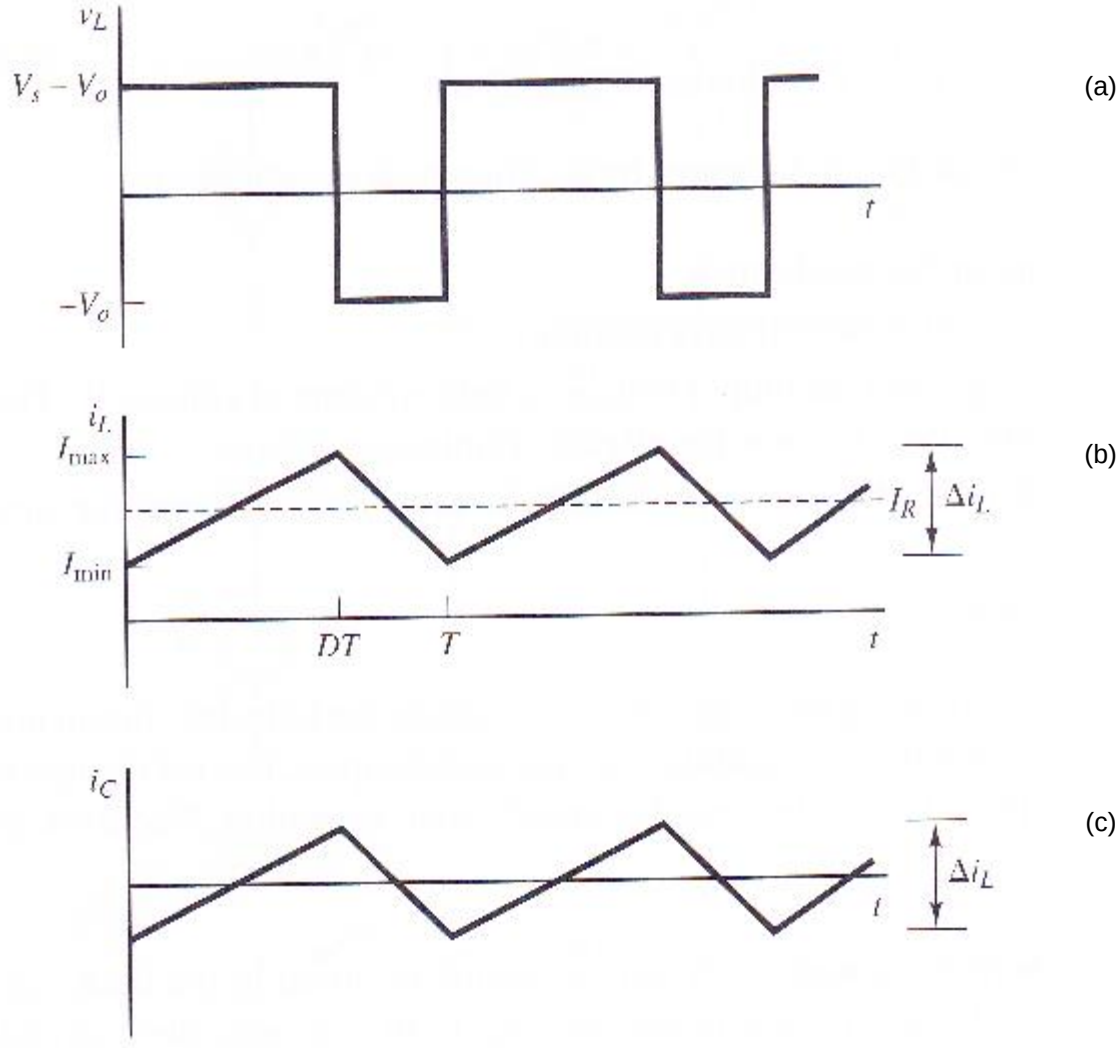

Figure 3.3 Buck converter waveforms. (a) Inductor voltage. (b) Inductor current. (c) Capacitor current.

3.1.2 Full Bridge

The full bridge converter, illustrated in figure 3.4 is a basic circuit used to convert DC to AC by closing and opening switches in proper sequence an ac output is created from a DC input. The output voltage v_o can be $+V_{dc}$, $-V_{dc}$, or zero, depending on which switches are closed.

Figure 3.4(b-e) illustrates the equivalent circuits for switching combinations. It is important that switches S1 and S4 or S2 and S3 not be closed at the same time. If the mentioned switches are closed a short circuit is created across the dc source. Also real switches do not turn off instantaneously; therefore a dead band must be placed in the control of the switches to prevent overlapping turn on [14].

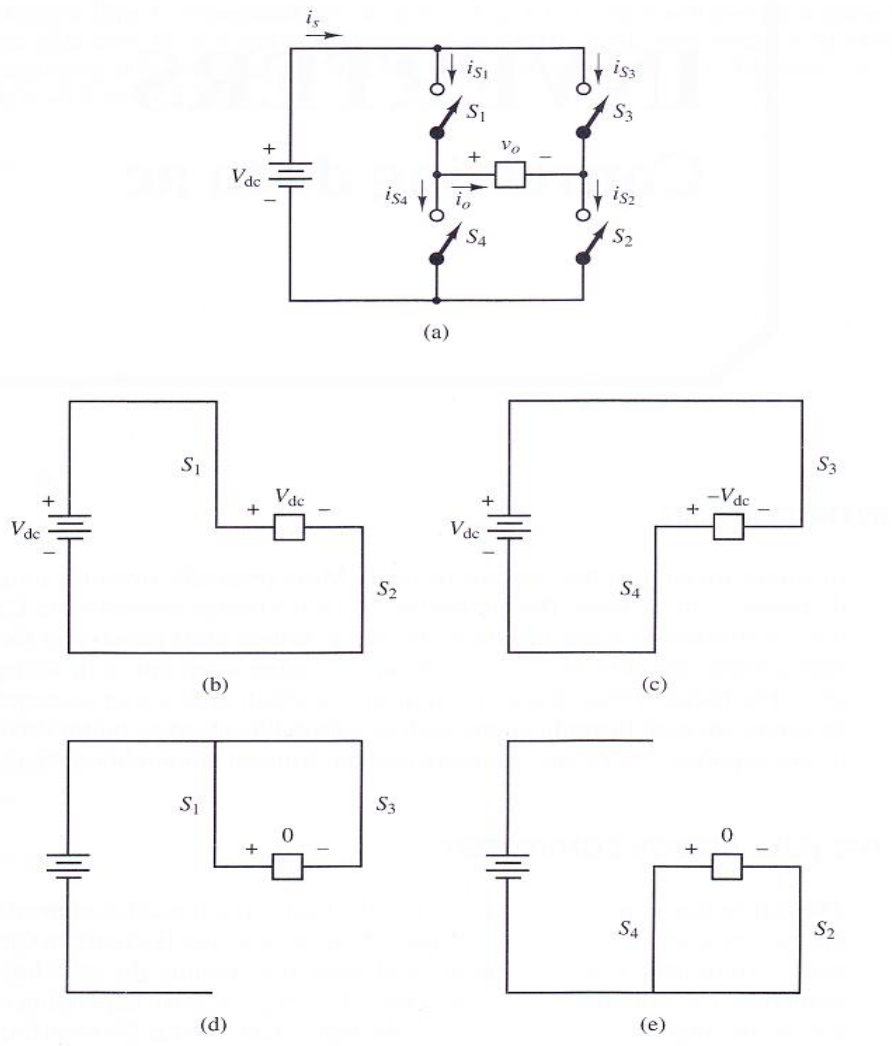

Figure 3.4 (a) Full bridge converter. (b) S1 and S2 closed. (c) S3 S4 closed. (d) S1 and S3 closed. (e) S2 and S4 closed.

The simplest switching scheme for the full bridge converter produces a square wave output voltage. The switches connect the load to $+V_{dc}$ when S_1 and S_2 are closed or to $-V_{dc}$ when S_3 and S_4 are closed. The periodic switching of the load voltage between $+V_{dc}$ and $-V_{dc}$ produces a square wave voltage across the load. Although this alternating output is non-sinusoidal, it may be an adequate ac waveform for some applications.

The current wave form in the load depends on the load components. For the resistive load, the current waveform matches the share of the output voltage. An inductive load will have a current that have more of a sinusoidal quality than the voltage because of the filtering property of the inductance. An induction load presents some considerations in designing the switches in the full bridge circuit because the switch currents must be bidirectional [14].

For a series R-L load and a square wave output voltage, assume switches S_1 and S_2 in figure xx a close at t=0. The voltage across the load is $+V_{dc}$, and current begins to increase in the load and in S_1 and S_2. The current in expressed as the sum of the forced and natural responses:

$$i_o(t) = i_f(t) + i_n(t) = \frac{V_{dc}}{R} + Ae^{-t/\tau}, \quad 0 \le t \le \frac{T}{2} \tag{3.12}$$

Where A is a constant evaluated from the initial condition and $\tau = {}^{L}/_{R}$.

At t=T/2, S_1 and S_2 open, and S_3 and S_4 close. The voltage across the R-L load becomes $-V_{dc}$, and the current has the form

$$i_o(t) = \frac{-V_{dc}}{R} + Be^{-(t-T/2)/\tau}, \quad \frac{T}{2} \le t \le T \tag{3.13}$$

Where B is evaluated from the initial condition.

When the circuit is first energized and the initial inductor current is zero, a transient occurs before the load current reaches a steady state condition. At steady state, i_o is periodic and symmetric about zero, as illustrated in figure xx. Let the initial condition for the current described in equation (3.12) be I_{min}, and let the initial condition for the current described in equation (3.13) be I_{max}.

Evaluating equation (3.12) at t=0,

$$i_o(0) = \frac{V_{dc}}{R} + Ae^0 \tag{3.14}$$

$$A = I_{min} - \frac{V_{dc}}{R} \tag{3.15}$$

Likewise, Equation (3.13) is evaluated at t=T/2:

$$i_o(T/2) = \frac{-V_{dc}}{R} + Be^0 = I_{max} \tag{3.15}$$

$$B = I_{max} + \frac{V_{dc}}{R} \tag{3.16}$$

In steady state, the current waveforms described by equation (3.12) and (3.13) then become

$$i_o(t) = \begin{cases} \frac{V_{dc}}{R} + \left(I_{min} - \frac{V_{dc}}{R}\right) e^{-t/\tau} & for\ 0 \le t \le \frac{T}{2} \\ \frac{-V_{dc}}{R} + \left(I_{min} + \frac{V_{dc}}{R}\right) e^{-(t-T/2)/\tau} & for\ \frac{T}{2} \le t \le T \end{cases} \tag{3.17}$$

An expression is obtained for I_{max} by evaluation the first part of equation (3.17) at t = T/2:

$$i(T/2) = I_{max} = \frac{V_{dc}}{R} + \left(I_{min} - \frac{V_{dc}}{R}\right) e^{-(T/2\tau)} \tag{3.18}$$

And, by symmetry,

$$I_{min} = -I_{max} \tag{3.19}$$

Substitution $-I_{max}$ for I_{min} in equation (3.18) and solving for I_{max},

$$I_{max} = -I_{min} = \frac{V_{dc}}{R}\left[\frac{1 - e^{-T/2\tau}}{1 + e^{-T/2\tau}}\right] \tag{3.20}$$

Thus, equation (3.17) and (3.20) describe the current in an R-L load in the steady state when a square wave voltage is applied [14].

3.1.3 Low Frequency Hardware

The experimental setup, shown in figure 3.5 shows the complete system which includes a power supply, driver board, buck converter and full bridge converter. Also a current sensor was added to the buck converter for better control of the arc.

A low frequency transformer was used as the first attempt to achieve high ac voltage output. The experiment is conducted with an off-the-shelf neon transformer operated at 500Hz. This topology can achieve 12kV peak ac voltage at the transformer secondary and the ac plasma can be generated at the operation frequency, the primary operation voltage and current is shown in Figure 3.6.

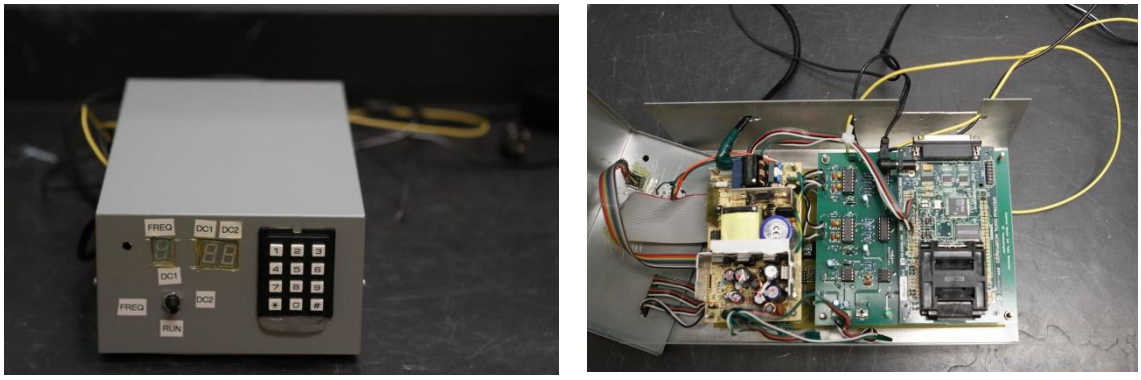

Figure 3.5 Buck convert and full bridge experiment hardware.

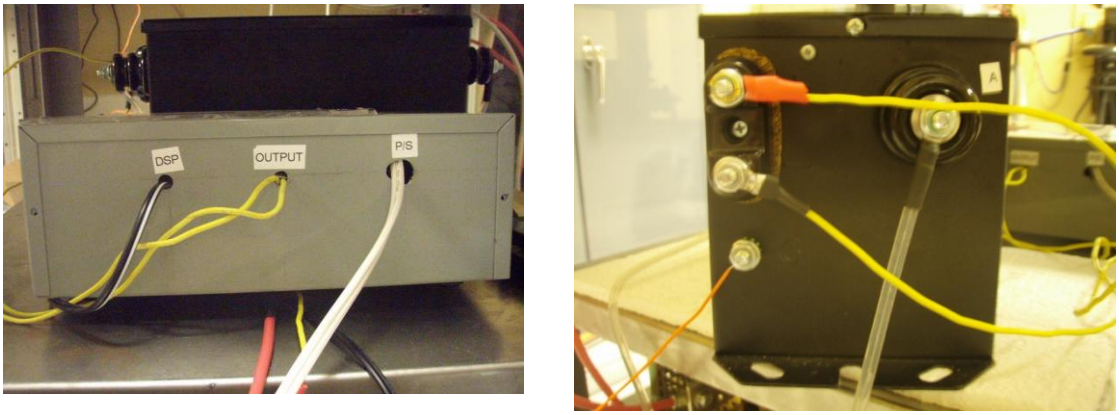

Figure 3.6 Buck converter and full bridge with the low frequency transformer.

Second phase of this project was to create a dial in frequency and duty cycle so different parameters could be tested on the cold plasma chamber for the highest yield of hydrogen. A four position switch was used to select between the frequency, and duty cycle, the frequency range is 1-9 kHz and duty cycle from 10%-99%. Figures 3.7(a)-(c) shows the hardware maturity from start to finish.

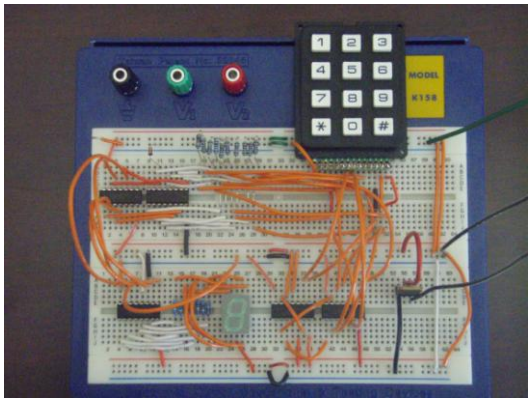

(a)

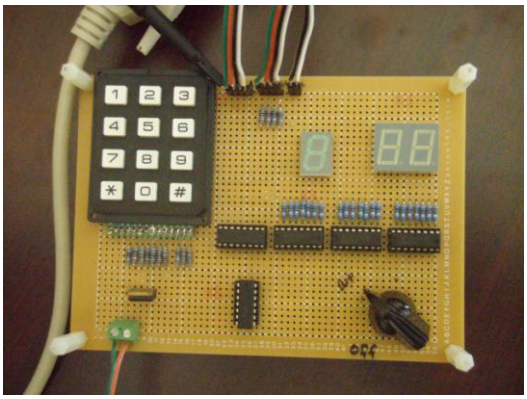

(b)

(c)

Figure 3.7 (a) Dial in frequency and duty cycle on bread board. (b) On proto board. (c) Implemented with the complete system.

3.1.4 High Frequency Transformer

The large size of the low frequency transformer was a problem, so the next step was to test a high frequency transformer shown in figure 3.8(right). High frequency transformer is smaller in size due to the reduction in the magnetic core. Since the system size and timing control are of concern, full bridge inverter with high frequency high voltage transformer is used. The system topology is the same as in Figure 3.5 with the transformer replaced by a higher frequency one.

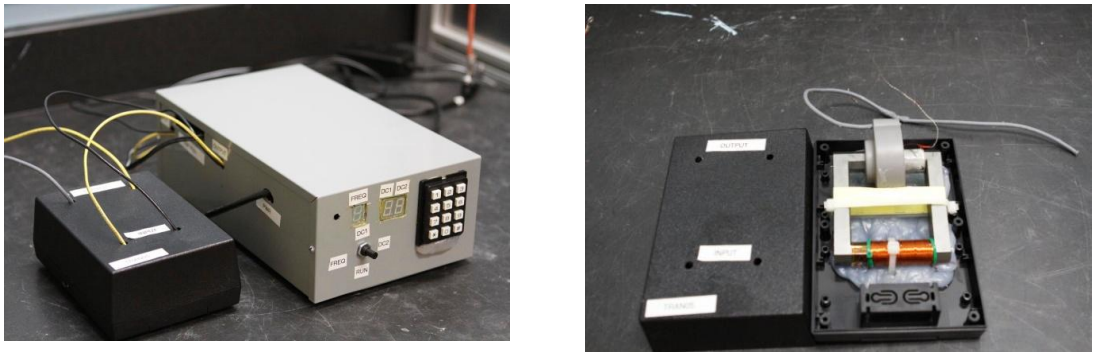

Figure 3.8 (left) Buck converter and full bridge connected to the high frequency transformers. (right) High frequency transformer.

3.2 Flyback Converter

The flyback converter illustrated in figure 3.9, is a dc/dc converter that provides isolation between input and output. An ideal transformer model that include the magnetizing inductance, Lm and the effects of losses and leakage inductances which are important when considering switch performance and protection. The general operation of the circuit is best understood with the simplified transformer model.

A few assumptions are made when analyzing the flyback converter.

- Output capacitor is very large, resulting in a constant output voltage, Vo.
- Circuit operates in steady state, implying all voltage and current periodic, starting and ending at the same point over one switching period.
- The duty ratio of the switch is D and is closed for time DT and open for (1-D)T.
- The switch and diode are ideal.

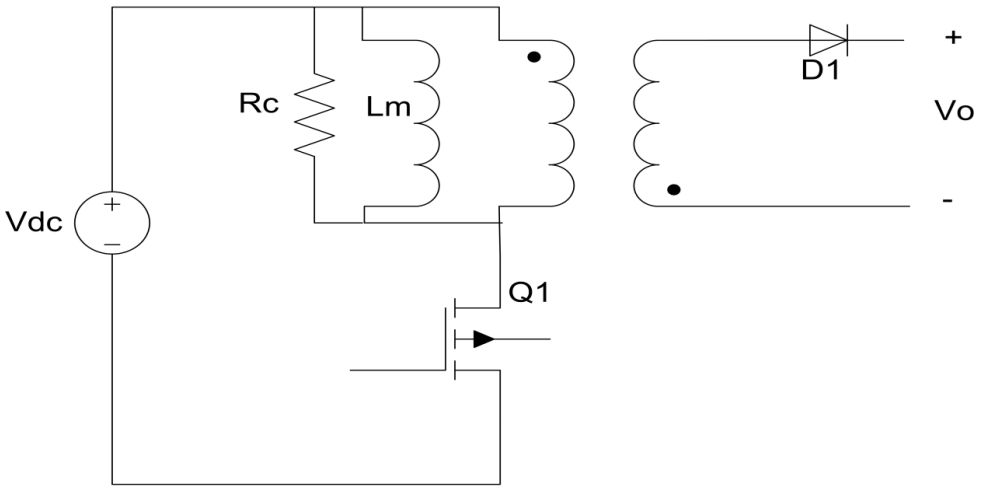

Figure 3.9 Flyback converter circuit.

The flyback converter operates by storing energy in Lm when the switch is closed and is then transferred to the load when the switch is open. The circuit is analyzed for both switch positions to determine the relationship between input and output.

When the switch is closed, the source side of the transformer:

$$v_1 = V_s = L_m \frac{di_{L_m}}{dt} \tag{3.14}$$

$$\frac{di_{L_m}}{dt} = \frac{\Delta i_{L_m}}{\Delta t} = \frac{\Delta i_{L_m}}{DT} = \frac{V_s}{L_m} \tag{3.15}$$

Solving for the change in current in the transformer magnetizing inductance,

$$\left(\Delta i_{L_m}\right)_{close} = \frac{V_s DT}{L_m} \tag{3.16}$$

On the load side of the transformer,

$$v_2 = v_1\left(\frac{N_2}{N_1}\right) = V_2\left(\frac{N_2}{N_1}\right) \tag{3.17}$$

$$v_D = -V_o - V_s\left(\frac{N_2}{N_1}\right) < 0 \tag{3.18}$$

Since the diode is off, $i_2 = 0$, which means that $i_1 = 0$. So while the switch is closed, current is increasing linearly in the magnetizing inductance Lm, and there is no current in the windings of the ideal transformer in the model. In an actually transformer, the current is increasing linearly in the physical primary winding, and no current exists in the secondary winding [14].

When the switch is open, the current cannot change instantaneously in the inductance Lm, so the conduction path must be through the primary turns of the ideal transformer. The current i_{L_m} enters the undotted terminal of the primary and must exit the undoted terminal of the secondary. This is allowable since the diode current is positive. Assuming that the output voltage remains constant at V_o, the transformer secondary voltage v2 becomes –Vo. The secondary voltage transforms back to the primary, establishing the voltage across Lm at

$$v_1 = -V_o \frac{N_1}{N_2} \tag{3.19}$$

Voltages and currents for an open switch are

$$v_2 = -V_o \tag{3.20}$$

$$v_1 = v_2 \frac{N_1}{N_2} = -V_o \frac{N_1}{N_2} \tag{3.21}$$

$$L_m \frac{di_{L_m}}{dt} = v_1 = -V_o \frac{N_1}{N_2} \tag{3.22}$$

$$\frac{di_{L_m}}{dt} = \frac{\Delta i_{L_m}}{\Delta t} = \frac{\Delta i_{L_m}}{(1-D)T} = -\frac{V_o}{L_m}\frac{N_1}{N_2} \tag{3.23}$$

Solving for the change in transformer magnetizing inductance with the switch open,

$$\Delta i_{L_{m\,open}} = \frac{-V_o(1-D)T}{L_m}\frac{N_1}{N_2} \tag{3.24}$$

Since the net change in inductor current must be zero over one period for steady-state operations, equations (3.16) and (3.24) show that

$$\Delta i_{L_{m\,closed}} + \Delta i_{L_{m\,open}} = 0 \tag{3.25}$$

$$\frac{V_s DT}{L_m} - \frac{-V_o(1-D)T}{L_m}\frac{N_1}{N_2} = 0 \tag{3.26}$$

Solving for Vo,

$$V_o = V_s \frac{D}{(1-D)} \frac{N_2}{N_1} \tag{3.27}$$

Other currents and voltages of interest while the switch is open are:

$$i_D = -i_1 \left(\frac{N_1}{N_2}\right) = i_{L_m} \left(\frac{N_1}{N_2}\right) \tag{3.28}$$

$$v_{Sw} = V_s - v_1 = V_s + V_o \left(\frac{N_1}{N_2}\right) \tag{3.29}$$

$$i_R = \frac{V_o}{R} \tag{3.30}$$

$$i_C = i_D - i_R = i_{L_m} \left(\frac{N_1}{N_2}\right) - \frac{V_o}{R} \tag{3.31}$$

Notice that v_{Sw}, the voltage across the open switch, is greater than the source voltage. If the output voltage is the same as the input and the turns ration is one, for example, the voltage across the switch will be twice the source voltage [14].

The power absorbed by the load resistor must be the same as that supplied by the source for the ideal case, resulting in

$$P_s = P_o \tag{3.32}$$

$$V_s I_s = \frac{V_o^2}{R} \tag{3.33}$$

The average source current I_s is related to the average of the magnetizing inductance current I_{L_m} by

$$I_s = \frac{(I_{L_m})DT}{T} = (I_{L_m})D \tag{3.34}$$

Substituting for I_s in equation (3.3) and solving for I_{L_m},

$$V_s I_{L_m} D = \frac{V_o^2}{R} \tag{3.35}$$

$$I_{L_m} = \frac{V_o^2}{V_s D R} \tag{3.36}$$

Using equation (3.27) for V_s, the average inductor current is also expressed as

$$I_{L_m} = \frac{V_s}{(1-D)^2 R}\left(\frac{N_2}{N_1}\right)^2 = \frac{V_o}{(1-D)R}\left(\frac{N_2}{N_1}\right) \tag{3.37}$$

The maximum and minimum values of inductor current are obtained from equation (3.16) and (3.37):

$$I_{L_m,max} = I_{L_m} + \frac{\Delta i_{L_m}}{2} = \frac{V_s D}{(1-D)^2 R}\left(\frac{N_2}{N_1}\right)^2 + \frac{V_s DT}{2L_m} \tag{3.38}$$

$$I_{L_m,min} = I_{L_m} - \frac{\Delta i_{L_m}}{2} = \frac{V_s D}{(1-D)^2 R}\left(\frac{N_2}{N_1}\right)^2 - \frac{V_s DT}{2L_m} \tag{3.39}$$

Continuous-current operation requires that $I_{L_m,min} > 0$ in equation (3.39). at the boundary between continuous and discontinuous current,

$$I_{L_m,min} = 0 \tag{3.40}$$

$$\frac{V_s D}{(1-D)^2 R}\left(\frac{N_2}{N_1}\right)^2 = \frac{V_s DT}{2L_m} = \frac{V_s D}{2L_m f} \tag{3.41}$$

Where f is the switching frequency and solving for the minimum value of L_m which will allow continuous current.

$$(L_m)_{min} = \frac{(1-D)^2 R}{2f}\left(\frac{N_1}{N_2}\right)^2 \tag{3.42}$$

So the output ripple voltage for the flyback is:

$$\frac{\Delta V_o}{V_o} = \frac{D}{RCf} \tag{3.43}$$

3.2.1 Flyback Hardware Setup

The second circuit used for this project was the flyback converter shown in figure 3.11. The dc power source was setup to take power from either a Sorenson power supply or from a 400W solar panel, using the buck converter to regulate any differences. A TMS320F2812 DSP from Texas Instrument was used to control the flyback switch, with a duty cycle of 70% and a frequency of 2kHz. The switch used for this project is rated for 600V and 24A. Since the rated power of the flyback transformer is only 20-25W, a parallel matrix of 8 flyback transformers was connected to divide the power.

In order to better expose the fuel to cold plasma, the electrodes configuration is plate to plate made of stainless steel. The experimental results are presented in Figure 3.10, where voltage slew rate of 1kv/μsec is achieved. The moments of plasma, where tremendous pulse

power is delivered within about 100ns period while almost negligible power is present during the rest of the switching period.

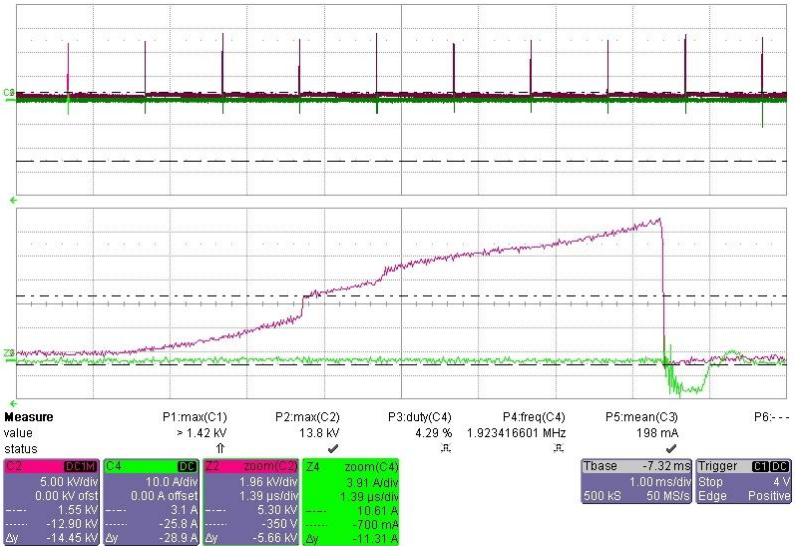

Figure 3.10 Flyback with arc showing rise time and fall time of the secondary voltage.

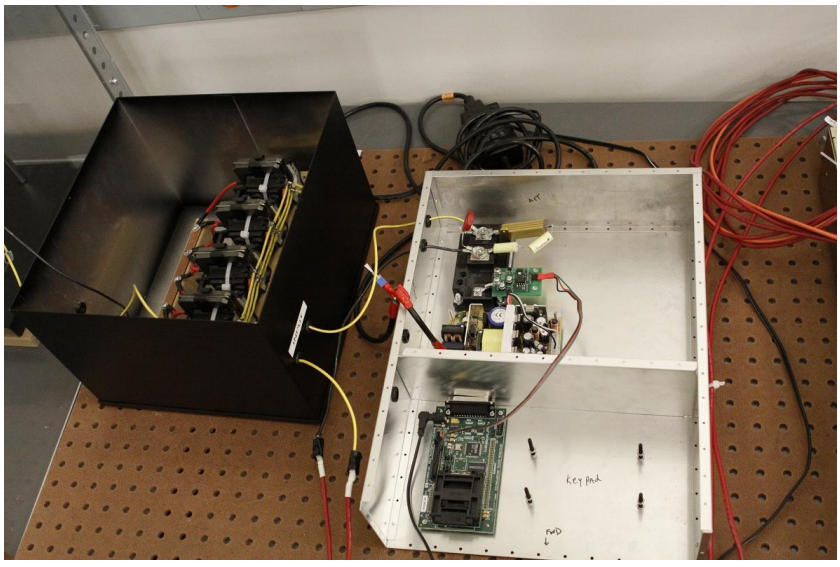

Figure 3.11 Flyback and transformer hardware.

CHAPTER 4

SUMMARY AND FUTURE WORK

Hydrogen has a high energy per mass but a lesser energy per volume than gasoline making it less attractive for transporting. Onboard fuel reforming of hydrocarbon for automotive application is one way to bypass the transporting and storage of hydrogen. The thesis objective is to create arc for the purpose of reforming ethanol inside a cold plasma chamber. The parameters of this project are to break a 10-15mm air-gap with a fuel mixture of 85% ethanol and 15% water per volume. To achieve this goal we started with a simple full bridge converter with a cascaded buck converter to control the input voltage. Designing the first prototype with an input voltage of 100V dc, and 200W, with a close loop control to control the arc and to identify the signature of the arc detection. Dial in frequency and duty cycle was developed to test what setup configuration yielded the most hydrogen. The initial tests were done on a low frequency 60HZ transformer but the size and weight were issues so the project moved to a high frequency transformer for compact size and lighter weight.

Creating an arc for reforming of hydrocarbon, need an instantaneous power with a resting period in between the arc for the reaction of fuel to take place. The second prototype developed was the flyback. This converter gave us the impulse of power and controllability of the arc to achieve the resting time for maximum yield of hydrogen. The flyback transformer was the second concern for this project. The high frequency and high voltage needed for creating cold plasma made it difficult to designing a flyback transformer. Voltage and current signals are

given at low power to explain the steady state and transient of the system, also a close up waveform of the voltage rise fall time is given to analysis the breakdown voltage of the cold plasma chamber.

4.1 Buck Converter and Full Bridge

Creating an arc across a 10-15mm air-gap to produce cold plasma; starting with the basic buck converter plus full bridge configuration with a low frequency transformer shown in figure 4.1

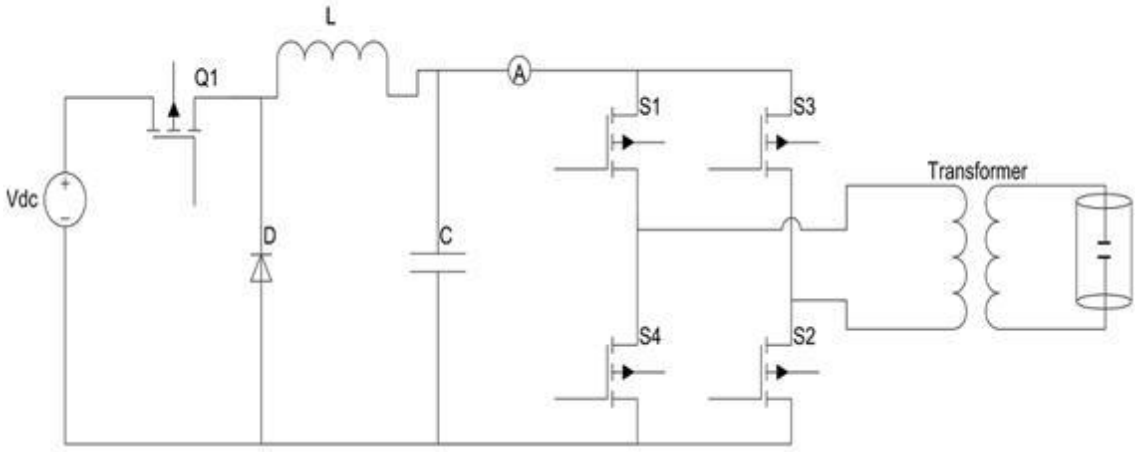

Figure 4.1 Buck converter plus inverter with a low frequency transformer schematic.

A current sensor was placed between the buck converter and full bridge to read the dc link current. The current signature was used to detect an arc inside the cold plasma chamber, if there was no arc the current waveform had a positive slope, and if there was an arc then the current waveform had a negative slope due to the negative impedance of plasma. Identifying the current signature for arc and no arc conditions, the buck converter was controlled to re-ignite the arc by increasing the duty cycle. Once the arc was establish the duty cycle was then reduced to conserve on power consumption.

4.2 Arc Detection

Since arcs can be lost due to parameter variations within the chamber, it is crucial to be able to detect the existence of the arc. Once arc loss is detected, the dc/dc converter will increase the voltage to re-ignite the gap. Figure 4.2 presents the foundation of our detection strategy. As can be noted, once the arc is established there will be negative-incremental impedance on the high voltage side of the transformer. This impedance which usually exhibits a large value (1 MΩ for a 15mm dry air gap), this impedance, once transferred to the low voltage side, will be added to the magnetizing inductance and core-loss resistance as shown in figure 4.2.

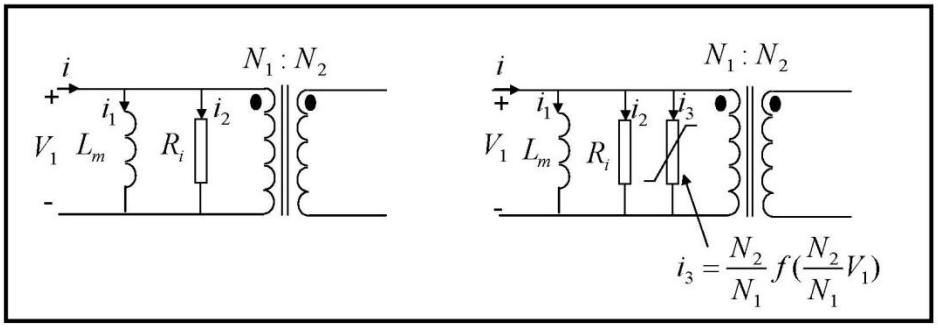

Figure 4.2 Ideal equivalent circuit of the high voltage/high frequency.

The time rate of change in input current to the transformer under no-arc and with arc conditions is expressed as follows:

No arc condition:

$$\frac{di}{dt} = \frac{V_1}{L_m} + \dot{V}_1 \frac{1}{R_i} + \left(\frac{N_s}{N_p}\right) C_{eq} \ddot{V} \tag{3.12}$$

In the presence of the arc:

$$\frac{di}{dt} = \frac{V_1}{L_m} + \dot{V}_1\left(\frac{1}{R_i} + \left(\frac{N_2}{N_1}\right)^2 \frac{df}{dV_1}\left(\frac{N_2}{N_1}V_1\right)\right) \approx \frac{V_1}{L_m} + \dot{V}_1\left(+\left(\frac{N_2}{N_1}\right)^2 \frac{df}{dV_1}\left(\frac{N_2}{N_1}V_1\right)\right) \tag{3.13}$$

In which V_1, L_m, R_i, N_2, N_1 and i represent primary (low voltage) voltage, magnetizing inductance, core-loss resistance, high voltage and low voltage turn numbers and primary current respectively. The nonlinear function $f(.)$ represents the negative admittance of the arc. At very high frequencies, the equivalent capacitances of the windings should be included. Furthermore, experiments have shown that the transferred impedance of the arc is much lower than the core-loss resistance, which makes it more significant than the core-loss resistance due to their parallel combination Due to negative increment impedance characteristic of the arc (i.e. $\frac{df}{dV} < 0$) one can conclude that there will be a significant change in the slope of the input current. In figure 4.3(a), (b) illustrates the change in current from a negative slope to a positive slope.

In fact our preliminary investigation shows that during commutation from positive/negative to negative/positive voltage levels the input dc-link current will exhibit a different profile during the existence of an arc as compared to no-arc condition. The commutation period can take up to a few microseconds. This is long enough for our digital monitoring based system to detect the change in the slope of the current. By continuously monitoring the current signature, one can note that in the absence of an arc, primary current tends to have an opposite sign as compared to the case when arc is established.

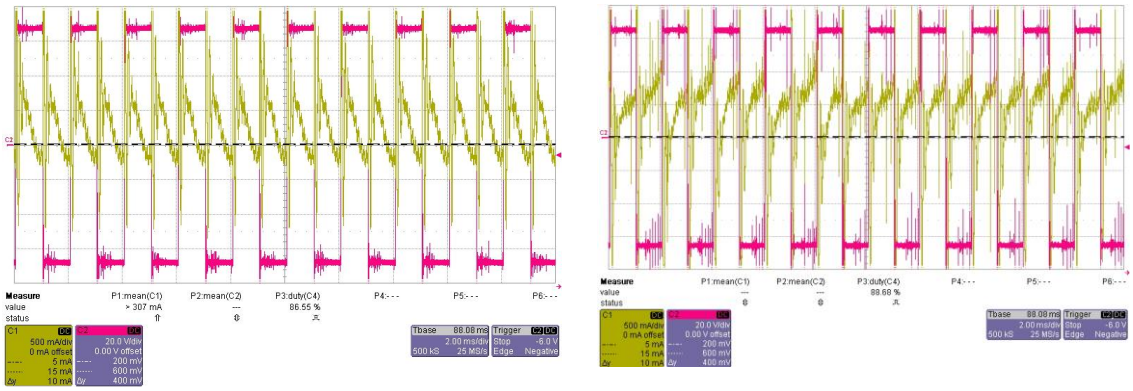

Figure 4.3 (left) Current signature in the absence of an arc, (right) current signature in the presence of an arc.

4.3 Low Frequency Transformer

An off the shelf 60 Hz transformer used for neon lighting was used for the first prototype. The turn ratio for the transformer is 1:125 step up with a maximum output voltage of 15kV. Figure 4.4 illustrates the primary voltage (red) and current (yellow) with the secondary side of the transformer open. The voltage is approximately 75V and the current is 1A with a frequency of 500Hz.

The initial test for creation and controlling the arc was a success. The current signature for arc detection proves to be a valuable tool to re-ignite the arc encases it is extinguish. The dial in frequency and duty cycle was a successful in reducing the amount of time for setting up to the next test. Also it provided a turnkey product for future use. The low frequency transformer was good in establishing the arc and test show the production of hydrogen but the mere size and weight of the transformer makes it unattractive for automotive use.

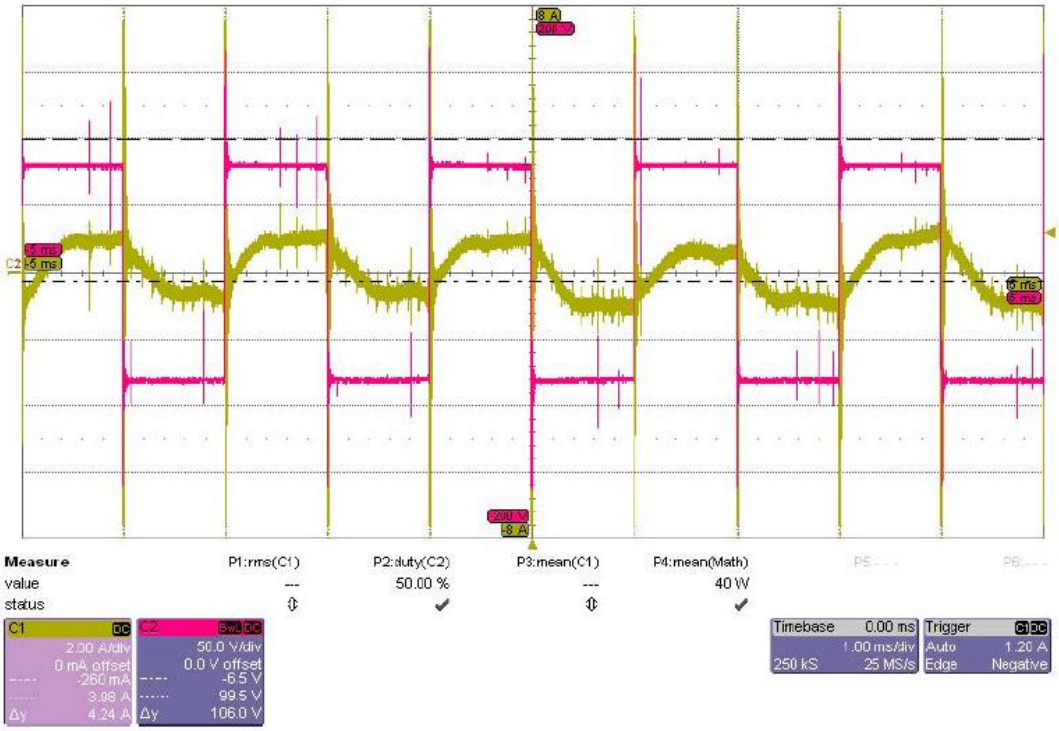

Figure 4.4 Low frequency full bridge converter primary voltage and current.

4.4 High Frequency Transformer

The size and weight of the lower frequency transformer was not applicable for automotive use. So three high frequency transformers were designed and tested for this project. The full bridge converter with high frequency high gain transformer can offer high bipolar peak voltage for plasma generation. The criteria for the high frequency transformer are 20kV output voltage, 200W and a magnetizing current of 1A. The size of the transformer was 5Hx4Wx4L. Figure 4.5 shows a load test of one of the high frequency transformer designed by a third party company. The primary voltage (green) shows a 75% duty cycle and the secondary voltage (red) shows 12kV output voltage. During the moment of plasma generation, the air gap is breakdown by high potential electric field and accumulated energy is released in the cold plasma chamber,

which only lasts for tens of nanoseconds. However, the observation from Figure 4.5 indicates that during the rest of the period, the reactive power still exists due to the parasitic capacitance of the high gain transformer. Therefore, the efficiency of the reformer is very low.

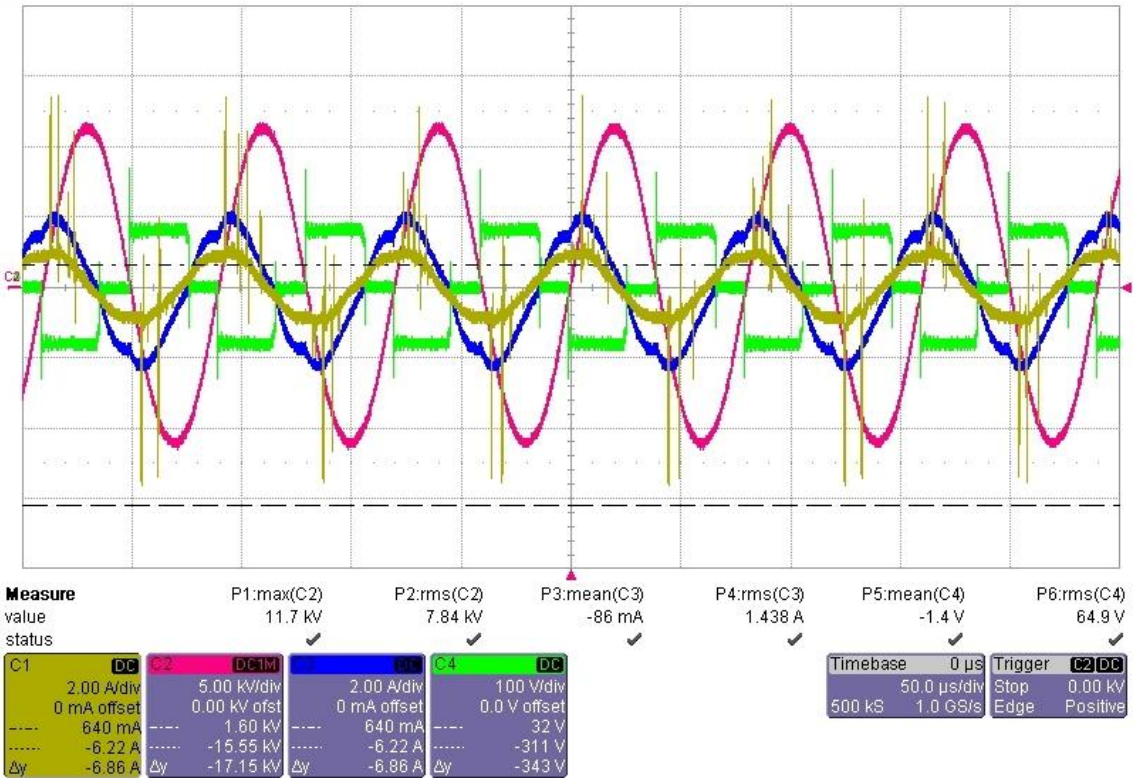

Figure 4.5 High frequency transformer results: 75% duty cycle with 12.5kHz switching frequency.

4.5 Flyback Converter

The second prototype used was the flyback converter. This objective was to create a pulse power supply for instantaneous voltage and current across the cold plasma electrodes. The high impulse voltage and current allowed for a high production of electronics and ions to form quickly and with enough kinetic energy to collide with the large molecules of ethanol and

water. This also allowed the control of the timing of the impulses to allow enough time for the reforming to take place within the chamber.

Flyback transformers are most commonly used in television sets. They are high voltage but low power (~20-25W). For this project we paralleled 8 flyback transformers to handle the 200W required to run the cold plasma reforming. Other attempts to design and build a specific transformer for this application was investigated but manufactures would not take on the project.

Figure 4.6 shows the primary and secondary, voltage and current. Notice the primary voltage (yellow) when the switch is on the voltage across the switch is zero and the current (red) starts to rise due to the storing of energy in the flyback transformer. When the switch turns off there is a voltage spike due to the inductance voltage in the transformer and the current on the primary side discharges over a short period of time. when the switch is opened on the primary side, the secondary side shows an instantaneous current (green) spike due to the capacitive nature of the cold plasma chamber with no arc and the voltage rises and discharges through ohmic loses in the transformer.

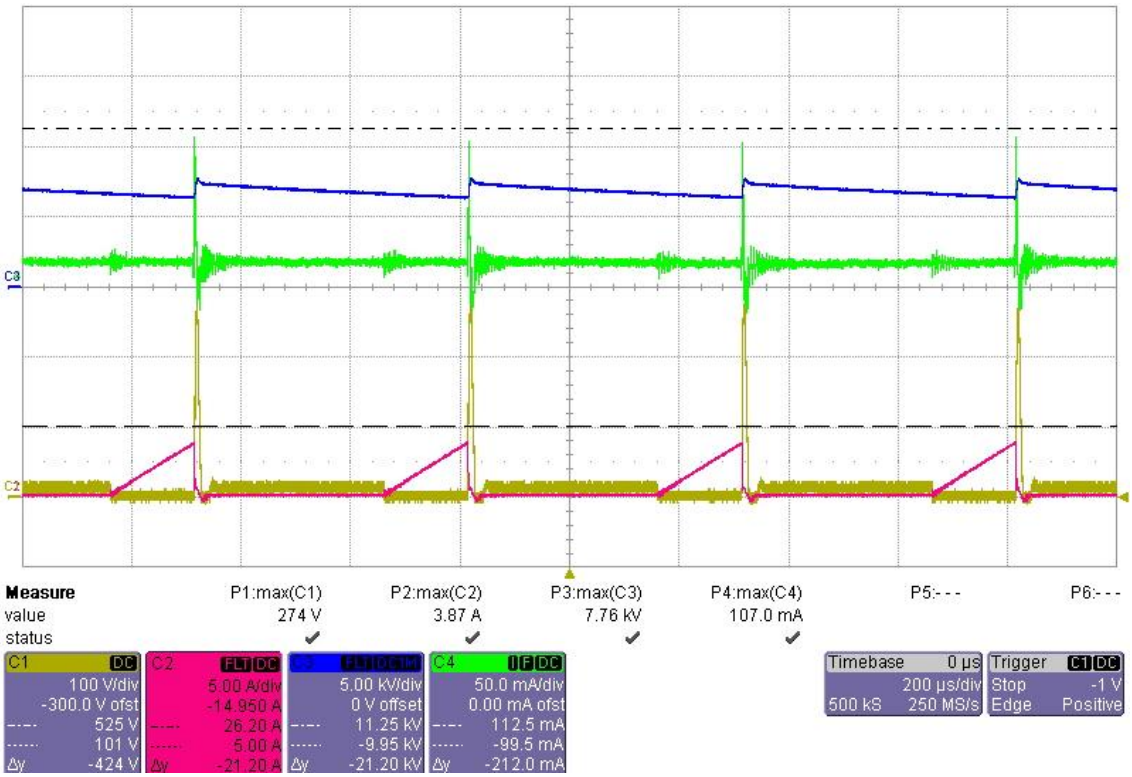

Figure 4.6 Flyback converter with no arc.

In figure 4.7 illustrates when there is arc across the electrodes. Again when the switch is closed the current rises due to the storing of energy in the transformer and when the switch is opened there is a voltage spike but the primary voltage does not go to the input voltage. It decays slowly. This voltage is due to the reflection of the secondary voltage (blue) to the primary voltage (yellow). On the secondary side, there is an instantaneous pulse of voltage and current due to the inductor of the transformer and the capacitance of the chamber. Once there is sufficient power is delivered to the chamber, an arc form causing a resistance across the electrodes allowing current to flow. The energy stored in the transformer dissipates to zero.

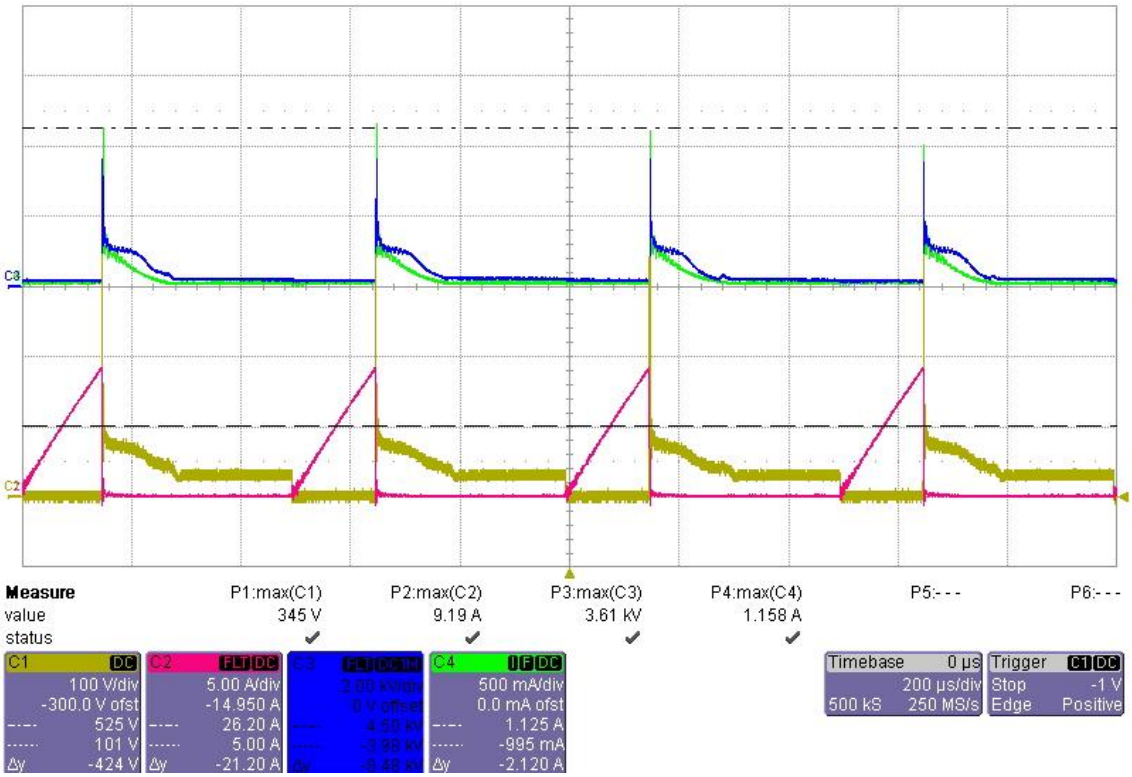

Figure 4.7 Flyback converter with arc.

The sample test was preformed with the air gap at 15mm, and a fuel flow rate of 2.5 mL/min. The electrical power input was 27W and hydrogen power output was 121W giving an ethanol to hydrogen ratio of 1:4.5, which is close to the theoretical ratio of 1:6.

4.6 Conclusion

The current trend of carbon dioxide emission, the transportation sector will be the main producer of green house gas. To help reduce the carbon dioxide emissions, onboard fuel reforming and onboard fuel enrichment is considered for automotive applications. Large scale

hydrogen production, such as steam reforming can produce large amounts of hydrogen but is not compatible with the automotive sector due it is size and weight limits.

In this thesis, the importance of cold plasma hydrogen reformer is addressed. In order to achieve effective plasma generation, high power density, and high efficiency, different converter topologies are investigated and evaluated with iterative experimental approaches. The pros and cons of each topology are discussed based on experimental evaluations; the low frequency transformer was the first prototype devolvement but the large size and weight of the transformer made it undesirable. The high frequency transformer was small and light weight but the parasitic capacitance made reforming inefficient. The flyback transformer and topology shows to be a good candidate for plasma reforming with pulse power and controllable timing between the arcs for maximum hydrogen yield. Overall, the flyback topology was chosen as the best power electronics topology, which overcomes the effect of transformer parasitic capacitance and delivers high power pulses to the reformer chamber.

4.7 Future Work

Plasma reforming shows promising results for hydrogen production but the unpredictability of the arc inside the chamber is an issue for a uniform and control of the plasma in the chamber. Controlling the cold plasma inside the reformer chamber by implementing a magnetic field around the chamber to control the arc and direct the arc in a more uniform pattern around the chamber may increase the production of hydrogen. As show in figure 4.8, using a set of four planar coils whose current waveforms are independently controlled, an external magnetic force will be exerted to the plasma. By precise control of the four magnetic forces the effective cross section of the arc will be maintained at an optimal level to increase the residence time and hence increase the productivity of the hydrogen.

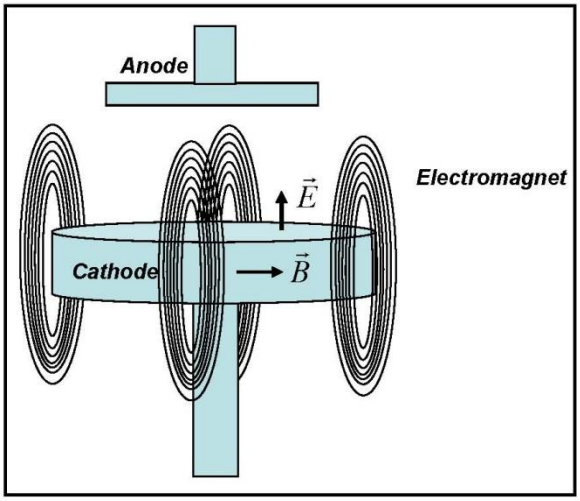

Figure 4.8 Schematic of magnetically enhanced plasma chamber.

REFERENCES

[1] Energy Information Administration, Internal Energy Outlook 2009," Office of Integrated Analysis and Forecasting, Tech. Rep. DOE/EIA-0484(2009).

[2] J.W Tester, E.M Drake, M.J. Driscoll, M.W Golay, and W.A. Peters, *Sustaninable Energy: Choosing Among Options.* Cambridge, MA: The MIT Press, 2005.

[3] Mehrdada Ehsani, Yimin Gao, Sebastien E. Gay, Ali Emadi, *"Modern Electric, Hybird Electric and Fuel Cell Vehicles"*, 2005".

[4] Xinli Zhu, Trung Hoang, Lance L. Lobban, Richard G. Mallinson, : Low CO Content Hydrogen production from Bio-Ethanol using a Combined Plasma Reforming-Catalytic Water Gas Shift Reactor", Applied Catalysis B: Environmental 94 (2010) 311-317.

[5] Amir Khoobroo, and Babak Fahimi, "On the efficiency of the fuel cell vehicles with onboard hydrogen generation" , IEEE Vehicle Pwer and Propulsion Conference, Sept. 2008.

[6] A. Grill, "*Cold Plasma in Material Fabrication, From Fundamental to Applications"* (New York: IEEE Press), 1994.

[7] M. Deminsky, V. Jivotov, B. Potapkin and V. Rusanov, "Plasma assisted production of hydrogen from hydrocarbons", Pure Applied Chem., 2002, 74(3), 413-418.

[8] G. Petitpas, J. D. Rollier, A. Darmon, J. Gonzalez-Aguilar, R. Metkemeijer and L. Fulcheri, "A comparative study of nonthermal plasma assisted reforming technologies", Int. Journal of Hydrogen Energy, 2007(32), 2848-2867.

[9] L. Bromberg, D. R. Cohn, A. Rabinovich and N. Alexeev "Hydrogen manufacturing using low current, non-thermal plasma boosted fuel converters", PSFC/RR-01-1, 2001.

[10] H. Conrads and M. Schmidt, "Plasma generation and plasma resources", Plasma Sources Sci. Tech., 2000(9), 441-454.

[11] A. Fridman, “Physics and Applications of the Gliding Arc Discharge”, IEEE conf. on Plasma Science, 2004, 410-411.

[12] S. Ahmed and M. Krumpelt, “Hydrogen from hydrocarbon fuels for fuel cells”, Int. Journal of Hydrogen Energy, 2001(26), 291-301.

[13] L. Bromberg, D. R. Cohn, A. Rabinovich and N. Alexeev, “Plasma catalytic reforming of methane”, Int. Journal of Hydrogen Energy, 1999(24), 1131-1137.

[14] Daniel W. Hart, *“Introduction to Power Electronics”*, Prentice-Hall, 1997.

BIOGRAPHICAL INFORMATION

Job Brunet was born in Houma, Louisiana in 1974. He has been a member of IEEE since 2004 and served as an IEEE officer and was Chair of IEEE, University of Texas at Arlington student branch from 2006-2007. He completed his undergraduate studies at the University of Texas at Arlington and received his B. S. degree in Electrical Engineering in August 2007. He continued on as a graduate student at the University of Texas at Arlington in order to work under Dr. Babak Fahimi in the Renewable Energy and Vehicular Motion Lab while pursuing his Masters degree in Electrical Engineering. His current research interests include Hydrogen Reforming, Battery Management Systems, Renewable Energy, and Power Electronics.